

Skyrmion quantum numbers and quantized pumping in two dimensional topological chiral magnets

Bohm-Jung Yang¹ and Naoto Nagaosa^{1,2,3}

¹*Correlated Electron Research Group (CERG), RIKEN Advanced Science Institute, Wako, Saitama 351-0198, Japan*

²*Department of Applied Physics, University of Tokyo, Tokyo 113-8656, Japan*

³*Cross-Correlated Material Research Group (CMRG), RIKEN Advanced Science Institute, Wako, Saitama 351-0198, Japan*

(Dated: October 20, 2018)

We investigate the general conditions to achieve the adiabatic charge and spin polarizations and quantized pumping in 2D magnetic insulators possessing inhomogeneous spin structures. In particular, we focus on the chiral ferrimagnetic insulators which are generated via spontaneous symmetry breaking from correlated two dimensional topological insulators. Adiabatic deformation of the inhomogeneous spin structure generates the spin gauge flux, which induces adiabatic charge and spin polarization currents. The unit pumped charge/spin are determined by the product of two topological invariants which are defined in momentum and real spaces, respectively. The same topological invariants determine the charge and spin quantum numbers of skyrmion textures. It is found that in noncentrosymmetric systems, a new topological phase, dubbed the topological chiral magnetic insulator, exists in which a skyrmion defect is a spin-1/2 fermion with electric charge e . Considering the adiabatic current responses of generic inhomogeneous systems, it is shown that the quantized topological response of chiral magnetic insulators is endowed with the second Chern number.

PACS numbers:

I. INTRODUCTION

After the seminal papers written by Jackiw and Rebbi¹ and Su, Schrieffer, and Heeger², quantum number fractionalization has become one of the most fundamental and fascinating concepts in condensed matter physics. For one dimensional spinless fermions, a domain wall soliton induces a localized mid-gap state which has a half of the electric charge. Later this idea is further generalized by Goldstone and Wilczek.³ Considering slow variations of the background mass fields in space and time, adiabatically induced currents are derived. The time component of the adiabatic current describes the charge density induced by the spatial variation of the mass soliton. The spatial integration of this charge density gives rise to the half electric charge.³ Moreover, the temporal variation of the background mass fields generates the spatial component of the adiabatic current, which describes the adiabatic charge polarization or even the quantized charge pumping.⁴ Therefore the existence of the topological soliton with nontrivial quantum numbers reflects the quantized dynamical response of the system.

The discovery of the time-reversal invariant spin Hall insulators⁵ has triggered great attentions to the two dimensional topological band insulators (TBIs). TBIs are the insulating phases that carry gapless edge states at the sample boundary due to the nontrivial bulk Berry phase, which can either break⁶ or preserve the time reversal symmetry.⁷ Because of the distinct bulk topological properties, π flux defects in TBIs carry nonzero spin or charge quantum numbers leading to Jackiw-Rebbi type topological solitons in two dimensional systems.⁸ In addition, in strongly interacting electron systems, it is proposed that TBIs can be obtained from the spontaneous breaking of spin rotation symmetry.⁹ Since this topological “Mott” insulator possesses a vector order parameter \hat{N} , skyrmion-type topological solitons are allowed, which are also expected to have nontrivial quantum numbers. For example, in the case of the spin Hall “Mott” insulator, a skyrmion defect is a boson

carrying a quantized electric charge $2e$.¹⁰

In this work, we focus on a different class of topological Mott insulators, the chiral magnetic insulators (CMIs), which can be obtained by considering electron-electron interactions in TBIs. In CMIs, the vector order parameter \hat{N} is given by the staggered spin ordering, which can acquire explicit time dependence by coupling to the external magnetic field. Because of the quantized charge and spin Hall effects, a skyrmion defect in CMIs can carry charge and spin quantum numbers satisfying fermionic or bosonic statistics depending on the magnitude of the bulk topological invariants. Considering smooth variations of the spin ordering directions in space and time, reminiscent of the approach pursued by Goldstone and Wilczek, we have shown that the quantized charge and spin pumpings are possible under the adiabatic change of the inhomogeneous spin structures such as the domain wall with rotating spins in collinear ferrimagnets or the conical ferrimagnetic phases in which the spatial modulation of the spin direction spreads over the whole system.

In CMIs, the quantum of the pumped charge/spin or the quantum number of a skyrmion strongly depends on the nature of the parent TBIs. In the case of the CMIs generated from the anomalous Hall insulator (AHI), the quantum of the pumped charge/spin is solely determined by the spin/charge Chern numbers of the collinear magnetic ground states. When the magnitude of the spin order parameter is small, the charge and spin Chern numbers are the same as those of AHI. In this case, the spin can be pumped in the unit of \hbar while the charge pumping is forbidden, which, at the same time, means that the skyrmion is a chargeless spin-1 boson. As the magnitude of the ordered spin moment increases, a new CMI phase dubbed the topological chiral magnetic insulator (TCMI) emerges in noncentrosymmetric systems, which supports a fermionic skyrmion with charge e and spin $\frac{\hbar}{2}$. Here the quantized charge and spin pumpings can be achieved.

On the other hand, in the case of CMIs derived from the spin Hall insulator (SHI), the spin anisotropy inherent to SHI

due to the spin-orbit coupling imposes constraints on the adiabatic pumping and skyrmion quantum numbers. The polarizations strongly depend on the relative orientation of the spin anisotropy and the magnetic ordering directions. When the spin order parameter is parallel to the spin anisotropy direction, the charge polarization induced by the rotating spins in domain walls is always zero. On the other hand, if the spin ordering is perpendicular to the spin anisotropy direction, finite charge polarization is expected for the Neel domain walls and the transverse conical spin states. In the case of a skyrmion, it does not carry a charge quantum number independent of the magnitude of the spin order parameter. However, a meron defect can be charged but the net charge is not quantized.

In addition, it is shown that the charge and spin polarizations in CMI can be understood in the framework of the adiabatic topological responses of generic inhomogeneous crystals.^{11–13} The inhomogeneity induced polarization current contains a topological part whose topological nature is endowed with the second Chern number, which is quantized in four dimensional closed manifolds. When the inhomogeneity is introduced by the spatially varying three-component unit vector \hat{N} , the inhomogeneity induced topological current can be separated into the homogeneous and inhomogeneous parts, which allows the second Chern number to be represented by the product of two independent topological invariants. One is the Chern number that is quantized in the momentum space and the other is the skyrmion number defined in the position/time spaces.

Since electron correlation effects are required to achieve CMI in addition to large spin-orbit coupling, transition metal oxides with 5d electrons can be an ideal platform to realize CMI. Recently, it is confirmed that the ground state of Sr_2IrO_4 is a spin-orbit entangled Mott insulator with anti-ferromagnetic spin ordering,^{14–17} which manifests the strong interplay of electron correlation and spin-orbit coupling effects in Ir-based compounds. In the case of Na_2IrO_3 which is expected to be SHI in non-interacting limit, anti-ferromagnetic spin ordering develops when electron correlation effects are included on the parent SHI phase.¹⁸ In this respect, Na_2IrO_3 is a candidate material in which the topological response of CMI can be observed. Moreover, it is recently proposed that bilayers of the perovskite-type transition metal oxides grown along the [111] direction can be potential candidates for two-dimensional topological insulators.^{19,20} The transition metal ions in the bilayer are located on a honeycomb lattice consisting of two trigonal sublattices on different layers. Interestingly, since the layer potential difference can be easily created by applying an electric field or by sandwiching the bilayer between two different substrates, lattice inversion symmetry can be explicitly broken in this system. Therefore to reveal the ground state of the bilayer systems, it is important to understand the interplay of the spin-orbit coupling, electron correlation, and the broken inversion symmetry.

The rest of the paper is organized in the following way. In Sec. II we construct a model Hamiltonian of CMIs taking into account electron-electron interactions in TBIs on the honeycomb lattice. Sec. III we consider the general conditions to achieve the quantized charge and spin pumpings through a

domain wall for CMI derived from AHI. The charge and spin quantum numbers of a skyrmion in CMI are also discussed. The investigation of the inhomogeneity induced charge polarization and skyrmion/meron quantum numbers is extended to CMI derived from SHI in Sec. IV. In Sec. V the adiabatic polarization currents for generic inhomogeneous systems are derived by using the semi-classical gradient expansion method. The topological origin of the quantized charge pumping in CMI is discussed from this viewpoint. Finally, we conclude in Sec. VI. The details of the procedures to derive the adiabatic polarization currents from the gradient expansion method are presented in Appendix A.

II. LATTICE MODEL OF TOPOLOGICAL CHIRAL MAGNETIC INSULATORS

The magnetic insulator with broken inversion symmetry is an ideal playground in which inhomogeneity induced responses can be investigated. This is because the lack of the spatial inversion symmetry allows Dzyaloshinskii-Moriya interaction which leads to spatially modulated spin structures. In this work, we focus on the magnetic insulators which can be obtained spontaneously from TBIs including inversion symmetry breaking terms. To demonstrate the main idea concretely, we start by constructing a model Hamiltonian of TCMI on the honeycomb lattice. Up to now, two types of TBIs are proposed on the honeycomb lattice. One is the anomalous Hall insulator (AHI) with broken time-reversal symmetry and the other is the time-reversal invariant spin Hall insulator (SHI). Starting from these TBIs, magnetic ordering can be developed when electron correlation is considered.¹⁸

The Hamiltonian describing the TCMI can be written in the following way,

$$\hat{H} = \hat{H}_1 + \hat{H}_2 + \hat{H}_U, \quad (1)$$

in which

$$\begin{aligned} \hat{H}_1 &= t_1 \sum_{\langle ij \rangle} \sum_{\sigma} [c_{i\sigma}^{\dagger} c_{j\sigma} + h.c.], \\ \hat{H}_2 &= \sum_i \mu_{S,i} c_i^{\dagger} c_i + \frac{i}{3\sqrt{3}} \sum_{\langle\langle ij \rangle\rangle} \sum_{\sigma=\uparrow,\downarrow} t_2(\sigma) c_{i,\sigma}^{\dagger} \hat{z} \cdot \hat{e}_{ij} c_{j,\sigma}, \end{aligned}$$

where $\langle ij \rangle$ and $\langle\langle ij \rangle\rangle$ denote the nearest-neighbor (NN) and next-nearest-neighbor (NNN) pairs, respectively. t_1 indicates the hopping amplitude between NN sites. $t_2(\sigma)$ is a spin independent constant $t_2(\sigma) = t_2$ in AHI while $t_2(\sigma) = t_2 (-t_2)$ for spin-up (spin-down) electrons in SHI, where t_2 is the amplitude of the pure imaginary hopping between NNN sites. The unit vector \hat{e}_{ij} is defined as $\hat{e}_{ij} = (\mathbf{d}_{ij}^1 \times \mathbf{d}_{ij}^2) / |\mathbf{d}_{ij}^1 \times \mathbf{d}_{ij}^2|$ where \mathbf{d}_{ij}^1 and \mathbf{d}_{ij}^2 are the bond unit vectors along the two bonds which are traversed by the electron when it moves from the site j to i . The noninteracting Hamiltonian \hat{H}_1 has a semi-metallic ground state at half-filling with two Dirac points at the momenta \mathbf{K}_1 and $\mathbf{K}_2 (= -\mathbf{K}_1)$. The staggered chemical potential $\mu_{S,i}$ in \hat{H}_2 , which breaks the lattice inversion symmetry, satisfies $\mu_{S,i} = \mu_S (-\mu_S)$ if i belongs to the A (B)

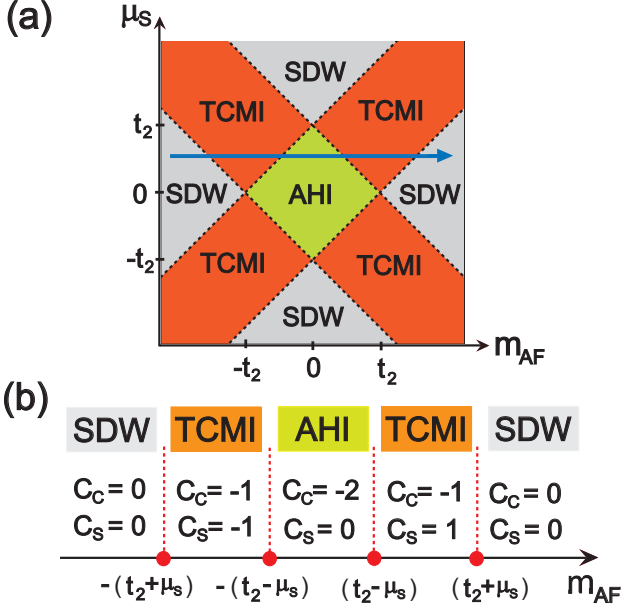


FIG. 1: (Color online) The schematic phase diagram of the full lattice mean field Hamiltonian \hat{H}_{Full} (Eq. (3)) for collinear magnetic phases derived from AHI. (a) The phase diagram shown in two dimensional space of (m_{AF}, μ_S) for given $t_2 > 0$. (b) One dimensional section of the 2D phase diagram, which is obtained by varying m_{AF} for given $t_2 > \mu_S > 0$ along the long arrow in (a). In both (a) and (b), a dotted line indicates the gapless phase boundary between gapped phases. In (b), each phase is characterized by the charge (C_C) and the spin (C_S) Chern numbers. Here TCMi (SDW) means a topological chiral magnetic insulator (spin density wave insulator).

sublattice. Considering the potential realization of CMI in bilayers of the perovskite-type transition metal oxides grown along the [111] direction, the inclusion of the staggered chemical potential $\mu_{S,i}$ is required.^{19,20} Interestingly, it is shown later that the existence of the inversion symmetry breaking term $\mu_{S,i}$ plays an essential role to stabilize TCMIs.

\hat{H}_U indicates electron-electron interactions generating a magnetic ground state. We introduce a collinear spin ordering along \hat{r} direction represented by $\mathbf{S}_A = m_A \hat{r}$ and $\mathbf{S}_B = m_B \hat{r}$ at the two sites A and B in a unit cell. Assuming the translational invariance of the magnetic ground state, the mean field approximation for \hat{H}_U leads to the following Hamiltonian,

$$\begin{aligned} \hat{H}_{\text{MF}} &= \sum_{\mathbf{k}} \sum_{i=x,y,z} \psi^\dagger(\mathbf{k}) [m_{F,i}(\tau_0 \sigma_i) + m_{\text{AF},i}(\tau_z \sigma_i)] \psi(\mathbf{k}), \\ &= \sum_{\mathbf{k}} \psi^\dagger(\mathbf{k}) [(\mathbf{m}_F \cdot \vec{\sigma}) + \tau_z (\mathbf{m}_{\text{AF}} \cdot \vec{\sigma})] \psi(\mathbf{k}), \end{aligned} \quad (2)$$

where $\psi^\dagger(\mathbf{k}) = (c_{A,\uparrow}^\dagger(\mathbf{k}), c_{A,\downarrow}^\dagger(\mathbf{k}), c_{B,\uparrow}^\dagger(\mathbf{k}), c_{B,\downarrow}^\dagger(\mathbf{k}))$. $\mathbf{m}_F = m_F \hat{r}$ and $\mathbf{m}_{\text{AF}} = m_{\text{AF}} \hat{r}$ with $m_F = (m_A + m_B)/2$ and $m_{\text{AF}} = (m_A - m_B)/2$. σ_i and τ_i ($i = x, y, z$) are Pauli matrices for spin and sublattice degrees of freedom and σ_0, τ_0 are identity matrices. Here $\sigma_i \tau_j \equiv \sigma_i \otimes \tau_j$ indicates a 4×4 matrix acting on the 4 component vector $\psi(\mathbf{k})$. Also

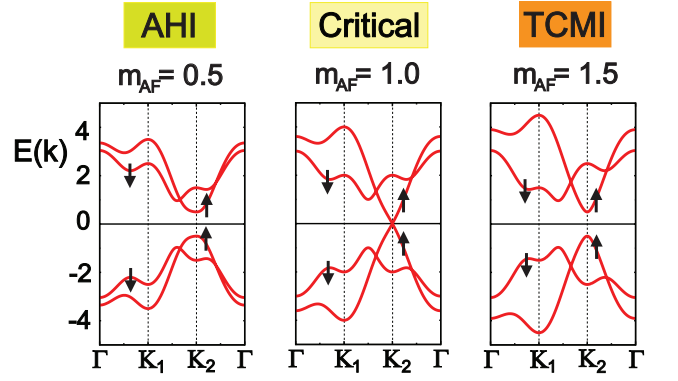


FIG. 2: (Color online) Evolution of the band structure as m_{AF} changes for $t_2 = 2, \mu_S = 1$. The AHI ($m_{\text{AF}} = 0.5$) turns into the TCMi ($m_{\text{AF}} = 1.5$) via a critical point at $m_{\text{AF}} = t_2 - \mu_S = 1$. Due to the broken time reversal and inversion symmetries, a band touching occurs only at $\mathbf{k} = \mathbf{K}_2$ between spin-up bands, which changes the charge and spin Chern numbers simultaneously.

when the direct product of Pauli matrices is involved with an identity matrix such as τ_0 or σ_0 , we omit the identity matrix in the product if the dimensionality of the Hamiltonian is obvious from the context. For example, $\tau_0 \sigma_i = \sigma_i$ in Eq. (2). Assuming $|m_{\text{AF}}| \gg |m_F|$, we first neglect the ferromagnetic component m_F , whose influence on the adiabatic polarization is considered later.

The full lattice mean field Hamiltonian can be written as

$$\hat{H}_{\text{Full}} = \hat{H}_1 + \hat{H}_2 + \hat{H}_{\text{MF}}, \quad (3)$$

which leads to the phase diagram shown in Fig. 1 and Fig. 3. The phase diagram is obtained in the following way. Since the (topological) phase transition between neighboring insulators occurs via band touching at $\mathbf{k} = \mathbf{K}_1$ or \mathbf{K}_2 , the phase diagram can be investigated by constructing the effective Hamiltonian describing the low energy particles near the two nodes $\mathbf{k} = \mathbf{K}_1$ or \mathbf{K}_2 . Explicitly, it is given by

$$H_{\text{low}}(\mathbf{q}) = q_x \tau_x \nu_z + q_y \tau_y + \mu_S \tau_z + t_2 \tau_z \nu_z \sigma'_\alpha + m_{\text{AF}} \tau_z \sigma_z, \quad (4)$$

where $\sigma'_\alpha = \sigma_0$ ($\sigma'_\alpha = \sigma_z$) for AHI (SHI). The Pauli matrices $\nu_{x,y,z}$ are introduced to indicate the node degrees of freedom, i.e., \mathbf{K}_1 ($\nu_z = 1$) and \mathbf{K}_2 ($\nu_z = -1$). The momentum (q_x, q_y) is measured with respect to the nodes. When the Hamiltonian can be written as a massive Dirac Hamiltonian such as $H = q_x \tau_x + q_y \tau_y + m \tau_z$, the sign reversal of the mass m changes the Chern number of the occupied band by $\Delta C = \text{sgn}(m)$ via a band touching at $m = 0$. Therefore the location of the phase boundary and the consequential change of Chern numbers can be understood by comparing the relative magnitude of μ_S, t_2 , and m_{AF} in Eq. (4). In addition, if the Chern number of one phase is known, the Chern numbers of all the other phases can be determined by investigating the sign change of the mass term of the effective Dirac Hamiltonian. For example, if $m_{\text{AF}} \gg t_2$ and $m_{\text{AF}} \gg \mu_S$, the corresponding gapped phase, i.e., the SDW phase, should have zero

Chern number since it is a topologically trivial. In this way, the phase diagrams in Fig. 1 and Fig. 3 can be obtained.

In addition, to confirm the structure of the phase diagram and topological property of each phase, the Chern number of each phase is numerically computed including the full band dispersion in the Brillouin zone. The Chern number C_σ of the occupied band with spin σ is defined as,

$$C_\sigma \equiv \frac{1}{2\pi} \int d^2k F_\sigma(\mathbf{k}), \quad (5)$$

where the momentum space Berry curvature $F_\sigma(\mathbf{k})$ is defined as $F_\sigma(\mathbf{k}) \equiv \partial_{k_x} A_{y,\sigma}(\mathbf{k}) - \partial_{k_y} A_{x,\sigma}(\mathbf{k})$ in which the Berry potential $A_{\mu,\sigma}(\mathbf{k})$ is given by $A_{\mu,\sigma}(\mathbf{k}) = -i \langle \Phi_\sigma(\mathbf{k}) | \partial_{k_\mu} | \Phi_\sigma(\mathbf{k}) \rangle$.^{21,22} Here $|\Phi_\sigma(\mathbf{k})\rangle$ indicates the periodic part of the Bloch wave function corresponding to the occupied state with spin σ .

Interestingly, various insulating magnetic phases with distinct topological properties are possible depending on the relative magnitudes of m_{AF} , t_2 , and μ_S . Different insulating phases are distinguished based on the Chern numbers obtained for the collinear magnetic ground states. Fig. 1 shows the magnetic ground states derived from AHI. Here we continue to use the term ‘‘AHI’’ as long as the magnetic phase possesses the charge Chern number $C_C = \pm 2$ and the spin Chern number $C_S = 0$. The charge (C_C) and spin (C_S) Chern numbers are defined as $C_C = C_\uparrow + C_\downarrow$ and $C_S = C_\uparrow - C_\downarrow$. In particular, for $||t_2| - |\mu_S|| < |m_{AF}| < |t_2| + |\mu_S|$, the TCMI, which can be characterized by the odd integer charge and spin Chern numbers ($|C_C| = |C_S| = 1$), is obtained. SDW indicates the magnetic insulator with $C_C = C_S = 0$.

The band structures of two topological phases, i.e., AHI and TCMI, and the band touching at the phase boundary between them are shown in Fig. 2. It is interesting to note that due to the broken time reversal and inversion symmetries, the band touching occurs only between spin-up bands at $\mathbf{k} = \mathbf{K}_2$. Since the Chern number for the occupied spin-up band changes by 1 ($\Delta C_\uparrow = 1$), the charge and spin Chern numbers also change simultaneously leading to TCMI phase.

In the case of magnetic insulators derived from SHI, the nature of the ground state depends crucially on the relative orientation between \mathbf{m}_{AF} and $\mathbf{t}_2 \equiv t_2 \hat{z}$. If $\mathbf{m}_{AF} \parallel \mathbf{t}_2$, i.e., $\mathbf{m}_{AF} = m_{AF} \hat{z}$, the phase diagram is shown in Fig. 3 (a) and (c). In this case, similar to the case of magnetic insulators derived from AHI, various topological insulators can be obtained depending on the relative magnitude of t_2 , μ_S , and m_{AF} . Here ‘‘SHI’’ also includes the magnetic phases which have the same Chern numbers as the usual nonmagnetic SHI phase assuming that the spin z component S_z is conserved. However, if S_z is not conserved, it is equivalent to a topologically trivial phase. As the relative angle between \mathbf{m}_{AF} and \mathbf{t}_2 increases, the phase boundaries between different gapped phases change. In particular, when $\mathbf{m}_{AF} \perp \mathbf{t}_2$, the area of TCMI phase shrinks to zero and the phase diagram contains only two phases, i.e., SHI and SDW. This is because when $\mathbf{m}_{AF} \perp \mathbf{t}_2$, in contrast to the case of $\mathbf{m}_{AF} \parallel \mathbf{t}_2$, gap-closing appears at the two nodes simultaneously along the phase boundary between SHI and SDW. In this case, the Chern number of the system does not change. The variation of the phase diagram as the relative angle between \mathbf{m}_{AF}

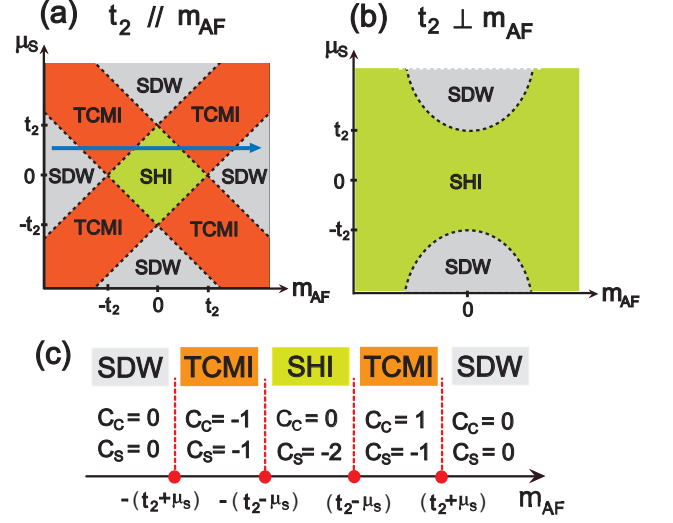


FIG. 3: (Color online) The schematic phase diagram of the full lattice mean field Hamiltonian \hat{H}_{Full} (Eq. (3)) for collinear magnetic phases derived from SHI. (a) The phase diagram shown in two dimensional space of (m_{AF}, μ_S) for given $t_2 > 0$ when $\mathbf{t}_2 \parallel \mathbf{m}_{AF}$. (b) The phase diagram for $\mathbf{t}_2 \perp \mathbf{m}_{AF}$. (c) One dimensional section of the 2D phase diagram, which is obtained by varying m_{AF} for given $t_2 > \mu_S > 0$ along the long arrow in (a). In (a), (b), (c), a dotted line indicates the gapless phase boundary between two gapped phases.

and \mathbf{t}_2 changes implies that starting from a TCMI phase with given \mathbf{t}_2 , μ_S , and \mathbf{m}_{AF} , if we rotate the direction of \mathbf{m}_{AF} relative to \mathbf{t}_2 , topological phase transitions should occur, through which TCMI turns into either SDW or SHI phase.

From the collinear magnetic states, the inhomogeneous spin structures can be introduced by considering smooth deformation of spin ordering directions. When the inversion symmetry breaking term μ_S is much smaller than the spin exchange couplings, the spins are aligned almost collinearly. In this limit, the local inhomogeneous spin structures, such as skyrmion defects and domain walls, can be developed. On the other hand, since the Dzyaloshinskii-Moriya interaction is allowed between localized spins when the inversion symmetry breaking term is finite, the inhomogeneous spin structure can be developed globally leading to spiral (or conical) spin orderings. All these inhomogeneous spin structures can be described by replacing $m_{AF} \hat{r} \cdot \vec{\sigma}$ with $m_{AF} \vec{\sigma} \cdot \hat{N}(\mathbf{r}, \eta)$ where the three-component unit vector \hat{N} is given by

$$\begin{aligned} \hat{N}(\mathbf{r}, \eta) &\equiv (N_x, N_y, N_z) \\ &= (\sin \theta(\eta) \cos \phi(\mathbf{r}), \sin \theta(\eta) \sin \phi(\mathbf{r}), \cos \theta(\eta)). \end{aligned} \quad (6)$$

For example, for $\mathbf{m}_{AF} = m_{AF} \hat{z}$, a static configuration with $\theta(\eta) = \theta(|\mathbf{r}|)$ satisfying the boundary conditions $\theta(|\mathbf{r}| = 0) = \pi$ and $\theta(|\mathbf{r}| \rightarrow \infty) = 0$, describes a skyrmion. Adopting $\phi(\mathbf{r}) = \tan^{-1}(\frac{y}{x})$, a skyrmion can be specified by the two parameters $(|\mathbf{r}|, \phi)$ which is nothing but the polar coordinates for two dimensional space. On the other hand, taking $\phi(\mathbf{r}) = \mathbf{Q} \cdot \mathbf{r}$ with proper boundary conditions, $\hat{N}(\mathbf{r}, \eta)$ describes a spiral

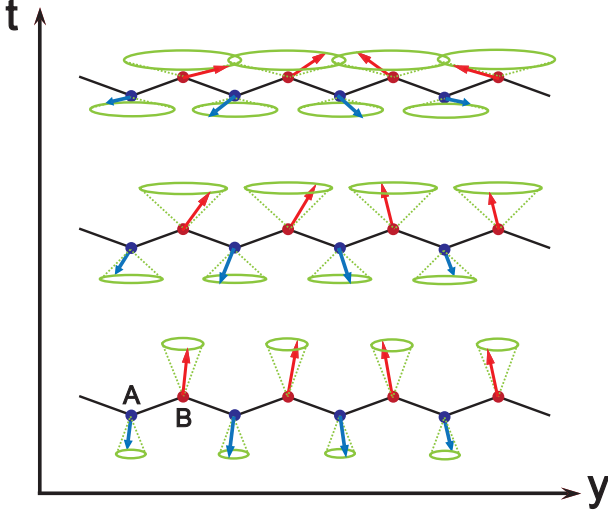


FIG. 4: (Color online) An example of the adiabatic variation of the inhomogeneous spin structure. A spiral spin state with the modulation wave vector $\mathbf{Q} = q\hat{y}$ is described. A pair of the spins at the two sublattice sites A and B are aligned in the opposite directions. The magnitude of the uniform component of the rotating spins is varying adiabatically (along the vertical direction in the figure), which can be controlled in experiment by applying external magnetic fields.

spin ordering with the modulation wave vector \mathbf{Q} or a smooth variation of spin directions around a domain wall.²³ In these cases, the spatial modulation itself can be described by a single parameter. For example, taking $\mathbf{Q} = Q\hat{y}$, $\phi(\mathbf{r}) = \phi(y)$ depends only on the y -coordinate. If we adopt the time coordinate t as η , $\hat{N}(y, t)$ describes the temporal variation of the inhomogeneous spin structures. Then $N_z = \cos\theta(t)$ denotes the uniform spin component independent of the spatial coordinates and the adiabatic variation of $\theta(t)$ controls the relative magnitude of the rotating and uniform spin components. In Fig. 4, we describe the adiabatic temporal change of the spiral ferrimagnetic ordering. Here the magnitude of the uniform component decreases as a function of t . It is the main purpose of this paper to understand the topological responses of the system due to the adiabatic change of the \hat{N} which varies in the two dimensional parameter spaces, either $(|\mathbf{r}|, \phi)$ or (y, t) .

III. TOPOLOGICAL RESPONSES OF CHIRAL MAGNETIC INSULATORS DERIVED FROM AHI

A. Effective action for the charge and spin responses

Let us first consider the charge and spin responses of CMIs which are derived from AHI. The low energy Hamiltonian, which is obtained by linearizing the energy spectrum of \hat{H}_{Full} near the two Dirac nodes, can be written as

$$H_{\text{eff}} = \int d^2r \psi^\dagger(\mathbf{r}, t) [(-i\partial_x)\tau_x\nu_z + (-i\partial_y)\tau_y + \mu_S\tau_z + t_2\tau_z\nu_z + m_{\text{AF}}\tau_z\hat{N}(\mathbf{r}, t) \cdot \vec{\sigma}] \psi(\mathbf{r}, t), \quad (7)$$

where the Fermi velocity of the Dirac particle is scaled to 1 and \hbar is set to 1. The corresponding action is given by

$$S = \int dt d^2r \psi^\dagger(\mathbf{r}, t) \gamma^t [(-i\gamma^\mu \partial_\mu) - i\mu_S - it_2\nu_z - im_{\text{AF}}\hat{N}(\mathbf{r}, t) \cdot \vec{\sigma}] \psi(\mathbf{r}, t), \quad (8)$$

where γ^μ ($\mu = t, x, y$) is defined as $(\gamma^t, \gamma^x, \gamma^y) = (-i\tau_z, \tau_y\nu_z, -\tau_x)$ and the summation over repeated indices is assumed throughout the paper.

We consider a local unitary transformation U satisfying $U^\dagger(\vec{\sigma} \cdot \hat{N})U = \sigma_z$, which rotates each spin to the $+z$ direction. Defining $\psi \equiv U\psi'$, the effective action can be written as

$$S = \int dt d^2r \psi'^\dagger(\mathbf{r}, t) \gamma^t [\gamma^\mu (-i\partial_\mu + A_\mu^C - \frac{1}{2}\vec{\sigma} \cdot \vec{B}_\mu) - i\mu_S - it_2\nu_z - im_{\text{AF}}\sigma_z] \psi'(\mathbf{r}, t), \quad (9)$$

where $\frac{1}{2}\vec{\sigma} \cdot \vec{B}_\mu \equiv iU^\dagger(\partial_\mu U)$, which shows that the inhomogeneous spin structure induces $SU(2)$ spin gauge fields in the rotated frame. The electromagnetic $U(1)$ gauge fields A_μ^C are introduced via minimal coupling and the electron charge $-e$ is set to -1. To derive the effective action for gauge fields, we split the action into two pieces $S = S_1 + S_2$ in which

$$S_1 = \int \frac{d^3k}{(2\pi)^3} \psi'^\dagger(k) G_0^{-1}(k) \psi'(k),$$

$$S_2 = \int \frac{d^3k}{(2\pi)^3} \frac{d^3q}{(2\pi)^3} \psi'^\dagger(k+q) \times \Delta_\mu(\partial_{k_\mu} G_0^{-1}) [eA_\mu^C(q) - \frac{1}{2}\vec{\sigma} \cdot \vec{B}_\mu(q)] \psi'(k), \quad (10)$$

where

$$G_0^{-1}(k) = \omega - [k_x\tau_x\nu_z + k_y\tau_y + \mu_S\tau_z + t_2\tau_z\nu_z + m_{\text{AF}}\tau_z\sigma_z]. \quad (11)$$

Here the three momenta k is defined as $k = (\omega, k_x, k_y)$ and $(\Delta_t, \Delta_x, \Delta_y) = (-1, 1, 1)$. The effective action can be obtained after integrating out the fermion fields and expanding the resulting action in powers of the gauge fields and their gradients. Straightforward calculation gives rise to the following expression for the effective gauge action,^{24,25}

$$S_{\text{eff}}[A_\mu^C, A_\mu^S] = \frac{C_C}{4\pi} \int dt d^2r \epsilon^{\mu\nu\lambda} A_\mu^C \partial_\nu A_\lambda^C + \frac{C_S}{4\pi} \int dt d^2r \epsilon^{\mu\nu\lambda} A_\mu^S \partial_\nu A_\lambda^C + \frac{C_C}{16\pi} \int dt d^2r \epsilon^{\mu\nu\lambda} A_\mu^S \partial_\nu A_\lambda^S, \quad (12)$$

where

$$C_C = \frac{\epsilon^{\mu\nu\lambda}}{24\pi^2} \int d^3k \text{Tr} [G_0 \frac{\partial G_0^{-1}}{\partial k_\mu} G_0 \frac{\partial G_0^{-1}}{\partial k_\nu} G_0 \frac{\partial G_0^{-1}}{\partial k_\lambda}],$$

$$C_S = \frac{\epsilon^{\mu\nu\lambda}}{24\pi^2} \int d^3k \text{Tr} [\sigma_z G_0 \frac{\partial G_0^{-1}}{\partial k_\mu} G_0 \frac{\partial G_0^{-1}}{\partial k_\nu} G_0 \frac{\partial G_0^{-1}}{\partial k_\lambda}], \quad (13)$$

which are nothing but the charge (C_C) and spin (C_S) first Chern numbers of the collinear magnetic ground state described by G_0 . The U(1) spin gauge field A_μ^S is defined as $A_\mu^S \equiv B_{\mu,z}$. It is straightforward to show that the fictitious spin gauge flux $F_{\mu\nu}^S \equiv \partial_\mu A_\nu^S - \partial_\nu A_\mu^S$ satisfies

$$F_{\mu\nu}^S = \partial_\mu A_\nu^S - \partial_\nu A_\mu^S = \hat{N} \cdot [(\partial_\mu \hat{N}) \times (\partial_\nu \hat{N})]. \quad (14)$$

The effective gauge action in Eq. (12) gives rise to the following expressions for the charge current,

$$\begin{aligned} j_\mu^C(r, t) &= \frac{\partial S_{\text{eff}}[A_\mu^C, A_\mu^S]}{\partial A_\mu^C(r, t)}, \\ &= \frac{C_C}{2\pi} \epsilon^{\mu\nu\lambda} \partial_\nu A_\lambda^C + \frac{C_S}{4\pi} \epsilon^{\mu\nu\lambda} \partial_\nu A_\lambda^S, \end{aligned} \quad (15)$$

and the spin current,

$$\begin{aligned} j_\mu^S(r, t) &= \frac{\partial S_{\text{eff}}[A_\mu^C, A_\mu^S]}{\partial A_\mu^S(r, t)}, \\ &= \frac{C_S}{4\pi} \epsilon^{\mu\nu\lambda} \partial_\nu A_\lambda^C + \frac{C_C}{8\pi} \epsilon^{\mu\nu\lambda} \partial_\nu A_\lambda^S. \end{aligned} \quad (16)$$

In the absence of the spin gauge flux $F_{\mu\nu}^S$, for example, for a homogeneous collinear magnetic ground state, the above charge and spin currents describe the usual quantized charge and spin Hall effects driven by the external electromagnetic fields. The magnitude of the quantized charge (spin) current is determined by the charge (spin) Chern number. On the other hand, if the spin gauge flux can be generated by space-time dependent variation of the order parameter \hat{N} through the relation in Eq. (14), the adiabatic charge and spin Hall currents flow in the absence of the electromagnetic fields. In this case, interestingly, the magnitude of the quantized charge (spin) current is determined by the spin (charge) Chern number in contrast to the case of the usual charge and spin Hall currents.

B. Charge and spin pumping through a domain wall with spiral spins

To demonstrate the idea of the spin gauge flux induced charge and spin responses, we consider the charge and spin polarizations induced by the adiabatic modulation of the spin direction in a domain wall of a CMI, which is described in Fig. 5(a). An in-phase domain wall can be represented by $\hat{N}(\mathbf{r}, \eta)$ in Eq. (6) with $\phi(\mathbf{r}) = \phi(y) = \frac{\pi}{2}[-1 - 2 \tanh(y/\ell_{\text{DW}})]$. For convenience, we rearrange the components of \hat{N} and consider $\hat{N} = \hat{N}_X(\mathbf{r}, t)$ given by

$$\hat{N}_X(\mathbf{r}, t) = (\cos \theta(t), \sin \theta(t) \cos \phi(y), \sin \theta(t) \sin \phi(y)), \quad (17)$$

where the spin x -component is uniform. Traversing the domain wall along the y direction, the spins rotate by 2π within the yz -plane. External time dependent magnetic field $\mathbf{H}(t) = H(t)\hat{x}$ coupled to the spins within the domain wall controls

the magnitude of the uniform (x) components of the rotating spins. We assume that the length scale of the domain wall ℓ_{DW} satisfies $\hbar v/E_g \ll \ell_{\text{DW}} \ll L_y$. Here L_y represents the system size along the y -direction, E_g is the bulk energy gap, and v is the typical velocity scale contained in the bulk band structure near the chemical potential. Therefore the spin modulation near the domain wall is smooth enough but, overall, the spins are aligned collinearly throughout the entire system in which the spin z component S_z can be treated as a conserved quantity.

Let us first consider the charge polarization induced by the spin gauge flux. From Eq. (14) and Eq. (15), the adiabatic charge polarization current is given by

$$\begin{aligned} j_\mu^C &= \frac{C_S}{8\pi} \epsilon^{\mu\nu\lambda} \hat{N} \cdot [(\partial_\nu \hat{N}) \times (\partial_\lambda \hat{N})], \\ &= \frac{C_S}{4\pi} \delta_{\mu,x} \hat{N} \cdot [(\partial_y \hat{N}) \times (\partial_t \hat{N})]. \end{aligned} \quad (18)$$

During the adiabatic evolution of $\theta(t)$ for $t \in [0, T]$, the spin electric field $E_y^S \equiv \partial_y A_t^S - \partial_t A_y^S = \hat{N} \cdot [(\partial_y \hat{N}) \times (\partial_t \hat{N})]$ produced by the spiral spins at the domain wall induces a charge current j_x^C , which leads to the average charge polarization $\langle P_x \rangle = \frac{1}{L_y} \int_0^{L_y} dy \int_0^T dt j_x^C$. In particular, if the unit vector $\hat{N}(y, t)$ fully covers the surface of the unit sphere in the (y, t) space during the adiabatic evolution, a quantized charge pumping is possible with the net charge transferred to the x direction given by

$$\begin{aligned} Q_{\text{pumped}} &= \int_0^T dt \int dy j_x^C \\ &= \frac{C_S}{4\pi} \int_0^\pi d\theta \int_{\pi/2}^{-3\pi/2} d\phi \hat{N} \cdot [(\partial_\phi \hat{N}) \times (\partial_\theta \hat{N})], \\ &\equiv C_S n_{\text{skyrmion}}, \end{aligned} \quad (19)$$

where n_{skyrmion} is the skyrmion number of the vector field $\hat{N}(y, t)$. Therefore the unit pumped charge is determined by the product of two topological invariants defined in momentum space (C_S) and position/time space (n_{skyrmion}).

Moreover, since an electron carries both charge and spin quantum numbers, a charge current accompanies a spin current simultaneously. The spin current induced by the adiabatic spin electric field can be understood in the following way. Since S_z is a good quantum number, a system with $(C_\uparrow, C_\downarrow) = (n_\uparrow, n_\downarrow)$ can be considered as a superposition of two subsystems with $(C_\uparrow, C_\downarrow) = (n_\uparrow, 0)$ and $(C_\uparrow, C_\downarrow) = (0, n_\downarrow)$, respectively. For given spin electric field E_y^S , the charge current induced in each subsystem should be $j_x^C = e \frac{(n_\uparrow)}{4\pi} E_y^S$ and $e \frac{(-n_\downarrow)}{4\pi} E_y^S$, respectively, considering the spin Chern number in each case. However, since the spin polarization directions are opposite in two subsystems, the total induced spin current is given by $j_x^S = \frac{\hbar}{2} \frac{(n_\uparrow)}{4\pi} E_y^S + (-\frac{\hbar}{2}) \frac{(-n_\downarrow)}{4\pi} E_y^S = \frac{\hbar}{2} \frac{(n_\uparrow + n_\downarrow)}{4\pi} E_y^S$. Therefore the amount of spin transfer is determined by the charge Chern number C_C . The adiabatic spin current induced by the spin gauge flux can be

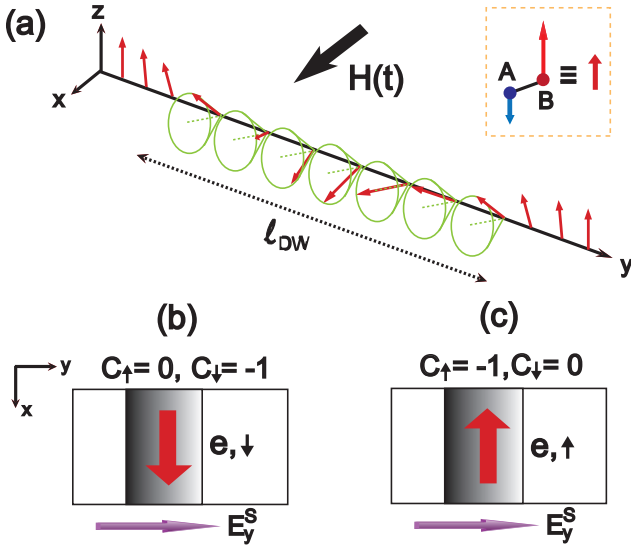


FIG. 5: (Color online) Charge and spin currents driven by the spin gauge flux which is produced by the slow variation of the uniform (x) component of the spins rotating in yz plane within a domain wall. (a) The rotating spins near the in-phase domain wall. Here the red rotating arrow describes the net ferromagnetic moment of a pair of the antiparallel spins within a unit cell. The external time dependent magnetic field $\mathbf{H}(t) = H(t)\hat{x}$ couples to the net ferromagnetic moment and controls the magnitude of the x -component of the rotating spins. In (b) and (c), the central square with graded colors in each panel, indicates the spiral domain wall producing the spin gauge flux on which the direction of the induced current is denoted with a red arrow. For a given spin gauge flux E_y^S , the direction of the adiabatic charge (spin) current is determined by the corresponding spin (charge) Chern number. (b) A TCMI with $(C_S, C_C) = (1, -1)$. (c) A TCMI with $(C_S, C_C) = (-1, -1)$.

written as

$$j_\mu^S = \frac{C_C}{16\pi} \epsilon^{\mu\nu\lambda} \hat{N} \cdot [(\partial_\nu \hat{N}) \times (\partial_\lambda \hat{N})]. \quad (20)$$

The identical expression of the spin current can also be obtained from Eq. (14) and Eq. (16). For an adiabatic cycle in which $\hat{N}(y, t)$ covers the full spherical solid angle, the net transferred spin along the x -direction is given by

$$\begin{aligned} S_{\text{pumped}} &= \int_0^T dt \int dy j_x^S \\ &= \frac{C_C}{8\pi} \int_0^\pi d\theta \int_{\pi/2}^{-3\pi/2} d\phi \hat{N} \cdot [(\partial_\phi \hat{N}) \times (\partial_\theta \hat{N})], \\ &= \frac{\hbar}{2} C_C n_{\text{skyrmion}}. \end{aligned} \quad (21)$$

Therefore the quantum of the pumped spin is determined by the product of the charge Chern number C_C and the skyrmion number n_{skyrmion} . Interestingly, the charge and spin responses under the spin gauge fields are exactly dual to the corresponding responses under the electromagnetic fields. Given the spin gauge fields, the charge (spin) response is determined by the spin (charge) Chern number.²⁴

In Fig. 5 (b) and (c), we show the adiabatic charge and spin currents induced by the adiabatic spin rotation at the spiral domain wall for the two TCMI with $C_S = 1$ and -1 in Fig. 1 (b). Interestingly, while the charge currents flow in the opposite directions because their C_S have opposite signs, the directions of the spin currents are the same in the two cases, consistent with the fact that $C_C = -1$ in both cases. Adiabatic charge and spin currents for AHI can be obtained by adding the corresponding currents for the two TCMI, i.e. by the superposition of Fig. 5 (b) and (c). Since the charge currents flow in the opposite directions, the net charge polarization is zero. However, the magnitude of the spin polarization is twice compared to the case of each TCMI.

C. Charge and spin quantum numbers of a skyrmion

It is worth noting that the last term of the effective gauge action in Eq. (12) is nothing but the Hopf term, which determines the spin and statistics of skyrmion solitons.²⁶ Therefore the topological invariants, which quantify the pumped spin and charge, also characterize the quantum numbers of skyrmion topological textures.²⁷ The time components of the adiabatic currents in Eq. (18) and Eq. (20) show the charge and spin densities associated with a skyrmion, which lead to the following expressions of the charge and spin quantum numbers of a skyrmion,

$$\begin{aligned} Q_{\text{skyrmion}} &= \frac{C_S}{4\pi} \int dx dy \hat{N} \cdot [(\partial_x \hat{N}) \times (\partial_y \hat{N})], \\ S_{\text{skyrmion}} &= \frac{C_C}{8\pi} \int dx dy \hat{N} \cdot [(\partial_x \hat{N}) \times (\partial_y \hat{N})]. \end{aligned} \quad (22)$$

Simple integration of the above equations shows that a skyrmion with the unit Pontryagin index on the TCMI is a spin-1/2 fermion with the charge $\pm e$. On the other hand, a skyrmion with the unit Pontryagin index on the AHI is a spin-1 boson with no electric charge. Therefore the skyrmion defects in TCMI and AHI carry nontrivial quantum numbers.

IV. TOPOLOGICAL RESPONSES OF CHIRAL MAGNETIC INSULATORS DERIVED FROM SHI

A. Effective action for the charge and spin responses

The low energy Hamiltonian of a CMI which is derived from the SHI is given by

$$\begin{aligned} H_{\text{eff}} &= \int d^2 r \psi^\dagger(\mathbf{r}, t) [(-i\partial_x)\tau_x \nu_z + (-i\partial_y)\tau_y \\ &\quad + \mu_S \tau_z + t_2 \tau_z \nu_z \sigma_z + m_{\text{AF}\tau_z} \hat{N}(\mathbf{r}, t) \cdot \vec{\sigma}] \psi(\mathbf{r}, t). \end{aligned} \quad (23)$$

In contrast to the case of CMI obtained from the AHI, the local $SU(2)$ spin rotation of the staggered spin order parameter $\hat{N}(\mathbf{r}, t)$ cannot make the Hamiltonian to be diagonal in spin

space because of the simultaneous rotation of the spin dependent t_2 term representing the strength of the spin-orbit coupling. To obtain the effective gauge action through the gradient expansion, it is necessary to transfer the position/time dependence of the Hamiltonian to the gauge fields via local unitary transformations, which can be achieved only in the limit of $|m_{\text{AF}}| \ll |t_2|$ or $|m_{\text{AF}}| \gg |t_2|$ corresponding to SHI or SDW phases in Fig. 3 (c), respectively. Therefore we focus on the adiabatic responses of SHI and SDW phases in the following discussion. Moreover, since the spin is not conserved in general due to the spin-orbit coupling, we only consider the charge polarization currents.

We first divide the Hamiltonian into two parts in such a way as $H_{\text{eff}} = H_{\text{eff},+} + H_{\text{eff},-}$ in which $H_{\text{eff},+}$ ($H_{\text{eff},-}$) corresponds to $\nu_z = 1$ ($\nu_z = -1$) describing the low energy particles near the node at $\mathbf{k} = \mathbf{K}_1$ ($\mathbf{k} = -\mathbf{K}_1$). Explicitly, $H_{\text{eff},\pm}$ are given by

$$H_{\text{eff},\pm} = \int d^2r \psi_{\pm}^{\dagger}(\mathbf{r}, t) [\pm(-i\partial_x)\tau_x + (-i\partial_y)\tau_y + \mu_S\tau_z + \tau_z\{\pm t_2\sigma_z + m_{\text{AF}}\hat{N}(\mathbf{r}, t) \cdot \vec{\sigma}\}] \psi_{\pm}(\mathbf{r}, t). \quad (24)$$

To make the Hamiltonian to be diagonal in spin space at each node separately, we define the collective spin degrees of freedom \hat{N}_{\pm} which combine $\hat{N} \cdot \vec{\sigma}$ and $t_2\sigma_z$ in the following way,

$$\begin{aligned} & \pm t_2\sigma_z + m_{\text{AF}}\hat{N}(\mathbf{r}, t) \cdot \vec{\sigma}, \\ & = m_{\text{AF}}N_x\sigma_x + m_{\text{AF}}N_y\sigma_y + (m_{\text{AF}}N_z \pm t_2)\sigma_z, \\ & \equiv \sqrt{m_{\text{AF}}^2 + t_2^2 \pm 2m_{\text{AF}}t_2N_z} \hat{N}_{\pm}(\mathbf{r}, t) \cdot \vec{\sigma}, \end{aligned} \quad (25)$$

where the new unit vector \hat{N}_{\pm} satisfies

$$\begin{aligned} & \hat{N}_{\pm} \cdot [(\partial_{\mu}\hat{N}_{\pm}) \times (\partial_{\nu}\hat{N}_{\pm})] \\ & = \frac{m_{\text{AF}}^2\{(m_{\text{AF}}\hat{N} \pm t_2\hat{z}) \cdot [(\partial_{\mu}\hat{N}) \times (\partial_{\nu}\hat{N})]\}}{[m_{\text{AF}}^2 + t_2^2 \pm 2m_{\text{AF}}t_2N_z]^{3/2}}. \end{aligned} \quad (26)$$

Now we consider the local unitary rotations U_{\pm} of the unit vectors \hat{N}_{\pm} satisfying $U_{\pm}^{\dagger}(\vec{\sigma} \cdot \hat{N}_{\pm})U_{\pm} = \sigma_z$. Defining $\psi_{\pm} \equiv U_{\pm}\psi'_{\pm}$, the effective action can be summarized as that in Eq. (10) but with G_0^{-1} replaced by

$$G_0^{-1}(k) = w - (\pm)k_x\tau_x - k_y\tau_y - \mu_S\tau_z - \sqrt{m_{\text{AF}}^2 + t_2^2 \pm 2m_{\text{AF}}t_2N_z}\tau_z\sigma_z, \quad (27)$$

and $\frac{1}{2}\vec{\sigma} \cdot \vec{B}_{\mu} \equiv iU_{\pm}^{\dagger}(\partial_{\mu}U_{\pm})$ or $iU_{\pm}^{\dagger}(\partial_{\mu}U_{\pm})$. In Eq. (27), G_0 depends on the position/time coordinates due to the presence of N_z term. Therefore when the variation of G_0 in the position/time spaces becomes important, the gradient of G_0 can also make a nontrivial contribution to the charge polarization as the gradient of the charge/spin gauge fields does. Therefore the effective gauge action approach in the previous section is valid only when $|m_{\text{AF}}| \ll |t_2|$ or $|m_{\text{AF}}| \gg |t_2|$ is satisfied, in which N_z has a negligible contribution to G_0 . However, regarding the charge polarization currents shown in Eq. (12) and Eq. (13), G_0 appears only in the definition of the Chern

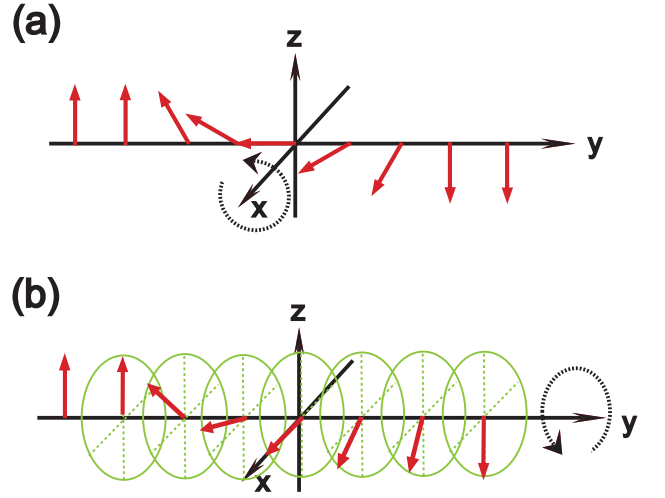


FIG. 6: (Color online) Spin structures at anti-phase domain walls for $\mathbf{m}_{\text{AF}} = m_{\text{AF}}\hat{z}$. Here the arrows indicate the staggered spins of the antiferromagnet (or ferrimagnet). Spins rotate with respect to an axis, \hat{x} or \hat{y} , which is normal to the collinear spin direction \hat{z} . (a) The Neel domain wall in which spins rotate around \hat{x} axis, normal to the spin modulation direction \hat{y} . The spin structure can be described by using \hat{N}_X^{DW} in Eq. (30). (b) The Bloch domain wall in which spins rotate around \hat{y} axis, parallel to the spin modulation direction. The spin structure can be described by using \hat{N}_Y^{DW} in Eq. (30).

number, which is topologically invariant. Therefore as long as N_z does not induce the change of the Chern numbers via band gap-closings, N_z dependence of G_0 does not affect the charge polarization current obtained by considering the gradients of gauge fields.

Through the gradient expansion of gauge fields following the same procedure as in Sec. III A, the adiabatic charge current can be obtained as

$$j_{\pm,\mu}^C(\mathbf{r}, t) = \frac{C_{S,\pm}}{8\pi} \varepsilon_{\mu\nu\lambda} \hat{N}_{\pm} \cdot [(\partial_{\nu}\hat{N}_{\pm}) \times (\partial_{\lambda}\hat{N}_{\pm})], \quad (28)$$

where $C_{S,\pm} = \mp 1$ for both $|m_{\text{AF}}| > ||t_2| + |\mu_S||$ and $|m_{\text{AF}}| < ||t_2| - |\mu_S||$ cases corresponding to SDW and SHI phases, respectively. The total charge polarization of the system can be obtained by adding the adiabatic currents from the two nodes,

$$j_{\mu}^C(\mathbf{r}, t) = j_{+,\mu}^C(\mathbf{r}, t) + j_{-,\mu}^C(\mathbf{r}, t). \quad (29)$$

The adiabatic charge polarization (and also the skyrmion charge) for arbitrary $|m_{\text{AF}}|$, especially for the TCMI phase corresponding to $||t_2| - |\mu_S|| < |m_{\text{AF}}| < ||t_2| + |\mu_S||$, is investigated in Sec. V by considering the systematic semiclassical expansion for adiabatic topological responses of inhomogeneous crystals.

B. Charge polarization at a domain wall with spiral spins

We consider the charge polarization or pumping through a domain wall with spiral spins. Because of the spin anisotropy

due to the spin-orbit interaction $\mathbf{t}_2 = t_2 \hat{z}$, the relative orientations of \mathbf{m}_{AF} , \mathbf{t}_2 , and the rotation axis of domain wall spins are crucial ingredients determining the charge polarization. To describe the domain wall spins, we consider the following representations of inhomogeneous spins,

$$\begin{aligned}\hat{N}_X^{\text{DW}}(\mathbf{r}, t) &= (\cos \theta(t), \sin \theta(t) \cos \phi(y), \sin \theta(t) \sin \phi(y)), \\ \hat{N}_Y^{\text{DW}}(\mathbf{r}, t) &= (\sin \theta(t) \sin \phi(y), \cos \theta(t), \sin \theta(t) \cos \phi(y)), \\ \hat{N}_Z^{\text{DW}}(\mathbf{r}, t) &= (\sin \theta(t) \cos \phi(y), \sin \theta(t) \sin \phi(y), \cos \theta(t)).\end{aligned}\quad (30)$$

In $\hat{N}_\alpha^{\text{DW}}$, the spin α -component is $\cos \theta(t)$ which is uniform independent of y . When we describe a domain wall with $\hat{N}_\alpha^{\text{DW}}$, α indicates the rotation axis of the domain wall spins. The deviation of θ from $\frac{\pi}{2}$ describes the adiabatic change of the relative magnitude of the uniform and rotating components of the domain wall spins.

In Fig. 6, anti-phase domain walls with rotating spins are described for $\mathbf{m}_{\text{AF}} = m_{\text{AF}} \hat{z}$. Here \hat{N}_X^{DW} with the boundary conditions of $\phi(y \rightarrow -\infty) = \frac{\pi}{2}$ and $\phi(y \rightarrow +\infty) = \frac{3\pi}{2}$, describes the Neel domain wall in which the spins rotate around \hat{x} -axis perpendicular to the spin modulation direction \hat{y} as shown in Fig. 6 (a). On the other hand, \hat{N}_Y^{DW} with the boundary conditions of $\phi(y \rightarrow -\infty) = 0$ and $\phi(y \rightarrow +\infty) = \pi$, describes the Bloch domain wall in which the spins rotate around the spin modulation direction \hat{y} as shown in Fig. 6 (b). For these two configurations we compute the partial polarization $\frac{dP_x}{d\theta}$ that is defined as

$$\frac{dP_x}{d\theta} = \int_{\phi(y \rightarrow -\infty)}^{\phi(y \rightarrow +\infty)} d\phi j_x^C(\theta, \phi). \quad (31)$$

Using Eq. (26), Eq. (28), and Eq. (29), it can be easily shown that $\frac{dP_x}{d\theta}$ for both \hat{N}_X^{DW} and \hat{N}_Y^{DW} are zero for any θ . Therefore no charge polarization occurs at the domain walls with rotating spins when $\mathbf{m}_{\text{AF}} \parallel \mathbf{t}_2$.

Similarly, the partial polarization $\frac{dP_x}{d\theta}$ induced by the rotating spins at the domain walls can be considered for $\mathbf{m}_{\text{AF}} \perp \mathbf{t}_2$. If $\mathbf{m}_{\text{AF}} \parallel \hat{x}$, \hat{N}_Z^{DW} (\hat{N}_Y^{DW}) describes the Neel (Bloch) domain wall with appropriate boundary conditions. It can be shown that $\frac{dP_x}{d\theta} \neq 0$ in general for the Neel domain wall (\hat{N}_Z^{DW}). On the other hand, in the case of the Bloch domain wall described by \hat{N}_Y^{DW} , $\frac{dP_x}{d\theta}$ has opposite signs for two inequivalent domain wall configurations in which $\phi(y) \in [-\frac{\pi}{2}, \frac{\pi}{2}]$ or $\phi(y) \in [\frac{\pi}{2}, \frac{3\pi}{2}]$, respectively. Therefore the average polarization for this case is expected to be zero when two anti-phase domain wall configurations are equally distributed in material. If $\mathbf{m}_{\text{AF}} \parallel \hat{y}$, both \hat{N}_X^{DW} and \hat{N}_Z^{DW} describe the Neel domain walls. For the Neel domain wall described by \hat{N}_Z^{DW} , $\frac{dP_x}{d\theta} \neq 0$ in general. However, in the case of the domain wall described by \hat{N}_X^{DW} , $\frac{dP_x}{d\theta}$ has opposite signs for two inequivalent domain wall configurations in which $\phi(y) \in [0, \pi]$ or $\phi(y) \in [\pi, 2\pi]$, respectively. The average polarization for this case is also expected to be zero.

Therefore the partial charge polarization $\frac{dP_x}{d\theta}$ can be nonzero only for $\mathbf{m}_{\text{AF}} \perp \mathbf{t}_2$ at the Neel domain walls described by \hat{N}_Z^{DW} . $\frac{dP_x}{d\theta}$ from the Neel domain wall is shown

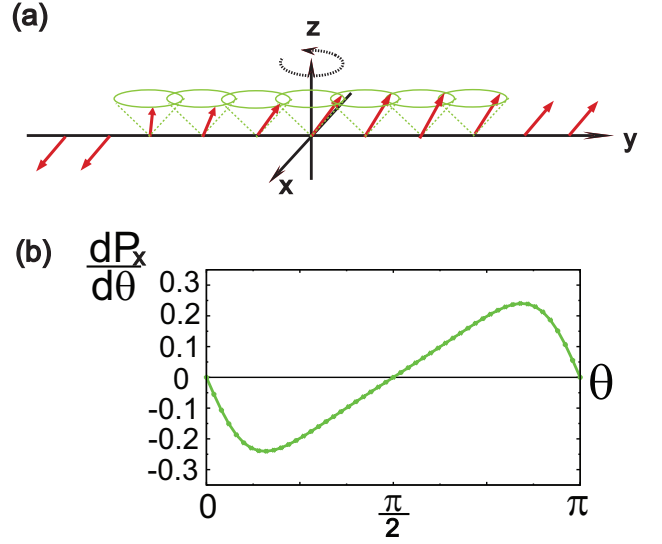


FIG. 7: (Color online) Charge polarization at the Neel domain wall described by $\hat{N}_Z^{\text{DW}} = (\sin \theta(t) \cos \phi(y), \sin \theta(t) \sin \phi(y), \cos \theta(t))$ for $\mathbf{m}_{\text{AF}} \parallel \hat{x}$. Here the boundary condition is given by $\phi(y \rightarrow -\infty) = 0$ and $\phi(y \rightarrow +\infty) = \pi$. (a) Spin configuration near the Neel domain wall. (b) $\frac{dP_x}{d\theta}$ as a function of θ .

in Fig. 7. Interestingly, if we assume that the spin rotation occurs over the whole lattice system, \hat{N}_Z^{DW} (\hat{N}_Y^{DW}) describes the transverse (longitudinal) conical magnetic ground state.²⁸ Therefore the charge polarization occurs only for the transverse conical magnetic phases in the direction perpendicular to the spatial modulation, consistent with the general theory for the charge polarization in spiral magnets.^{23,29}

Now let us discuss about the quantized charge pumping (also the charge quantum number of a skyrmion) considering the variations of $\phi \in [0, 2\pi]$ and $\theta(t) \in [0, \pi]$. At first, for \hat{N}_Z^{DW} , the local adiabatic charge currents $j_{\pm, x}^C(\mathbf{r}, t) = j_{\pm, x}^C(\theta, \phi)$ can be obtained, which satisfy the following relations,

$$j_{-, x}^C(\theta, \phi) = -j_{+, x}^C(\pi - \theta, \phi). \quad (32)$$

Because of this relation, the total charge current $j_x^C(\theta, \phi) = j_{+, x}^C(\theta, \phi) + j_{-, x}^C(\theta, \phi)$ also satisfy the following condition,

$$j_x^C(\theta, \phi) = -j_x^C(\pi - \theta, \phi). \quad (33)$$

Therefore if the uniform component $N_z = \cos \theta(t)$ of $\hat{N}(\mathbf{r}, t)$ changes over the full polar angle $\theta(t) \in [0, \pi]$, the net transferred charge due to the adiabatic charge current j_x^C is zero, i.e.,

$$Q_{\text{pumped}} = \int_0^T dt \int dy j_x^C = 0. \quad (34)$$

On the other hand, for $\hat{N}_X^{\text{DW}}(\mathbf{r}, t)$ and $\hat{N}_Y^{\text{DW}}(\mathbf{r}, t)$, it can be shown that the adiabatic charge polarization is always zero for any given $\theta(t)$ after the integration over ϕ , because of the

following condition satisfied by $j_{x,\pm}^C(\theta, \phi)$,

$$j_{x,+}^C(\theta, \phi) = -j_{x,-}^C(\theta, \phi + \pi). \quad (35)$$

Therefore the quantized charge pumping is impossible for any orientation of \mathbf{m}_{AF} .

The fact that the net transferred charge is zero can be understood in terms of the spin gauge flux induced spin Hall effect. If $|m_{\text{AF}}| \gg |t_2|$ where \hat{N}_+ and \hat{N}_- are almost parallel, the charge current density is proportional to $C_{S,+} + C_{S,-}$ as shown in Eq. (28) and Eq. (29). Since $C_{S,+} = -1$ and $C_{S,-} = 1$ in this limit, the total charge current is zero for given spin gauge flux. The opposite sign of $C_{S,\pm}$ is the direct consequence of the fact that the Dirac particles at the two nodal points have the opposite winding directions, which is reflected in the opposite sign of the k_x dispersions in Eq. (24).^{30,31} However, when $|m_{\text{AF}}|$ is finite, \hat{N}_+ and \hat{N}_- are tilted with a small relative angle due to the spin-orbit coupling. In this case, since the spin gauge fluxes generated by \hat{N}_\pm are different, the local polarization current can be nonzero although $C_{S,+} = -1$ and $C_{S,-} = 1$ are still satisfied. Therefore the finite partial polarization $\frac{dP_x}{d\theta}$ is essentially the result of the spin anisotropy due to the spin-orbit coupling, not of a topological origin. On the other hand, if $|m_{\text{AF}}| \ll |t_2|$ corresponding to SHI phase, the solid angle subtended by \hat{N}_\pm is very tiny even though \hat{N} covers the full spherical solid angle, which leads to vanishingly small charge polarization. The quantized pumping is also impossible in SHI case.

C. Skyrmion charge

The skyrmion defects of the collinear magnetic phases satisfying $\mathbf{m}_{\text{AF}} \parallel \mathbf{t}_2$ or $\mathbf{m}_{\text{AF}} \perp \mathbf{t}_2$ can also be described by using the spin configurations $\hat{N}_{X,Y,Z}^{\text{DW}}$ in Eq. (30). For the description of a skyrmion, we replace $\theta(t)$ by $\theta(|\mathbf{r}|)$ satisfying the boundary conditions $\theta(|\mathbf{r}| = 0) = \pi$ and $\theta(|\mathbf{r}| \rightarrow \infty) = 0$ and adopt $\phi(\mathbf{r}) = \tan^{-1}(\frac{y}{x})$ with $\mathbf{r} = (x, y)$. In the case of $\mathbf{m}_{\text{AF}} \parallel \mathbf{t}_2$, a skyrmion defect can be described by using \hat{N}_Z^{DW} . As Eq. (31), Eq. (33) and Fig. 7 (b) show, the adiabatically induced charge of a skyrmion, which is equivalent to the partial polarization of a domain wall, is anti-symmetrically distributed with respect to $(\theta - \pi/2)$. Therefore the integration of the induced charge adds up to zero, which shows that the skyrmion is not charged. On the other hand, when $\mathbf{m}_{\text{AF}} \perp \mathbf{t}_2$, a skyrmion can be described by \hat{N}_X^{DW} or \hat{N}_Y^{DW} . In this case, as shown in Eq. (35), the induced charge is zero for any θ value. Therefore the skyrmion is not charged.

To sum up, the skyrmions in CMIs derived from SHI do not carry the charge quantum number at least for $|m_{\text{AF}}| < ||t_2| - |\mu_S||$ or $|m_{\text{AF}}| > |t_2| + |\mu_S|$, which corresponds to SHI or SDW phases, respectively.

D. Meron charge

The anti-symmetric distribution of the induced charge with respect to $(\theta - \pi/2)$, shown in Fig. 7 (b), implies that a meron-

type defect in which θ changes over $\theta \in [0, \pi/2]$ can be charged although a skyrmion is chargeless. For $\mathbf{m}_{\text{AF}} \parallel \mathbf{t}_2$, a meron can be described by \hat{N}_Z^{DW} with the boundary condition given by $\theta(|\mathbf{r}| = 0) = \pi/2$ and $\theta(|\mathbf{r}| \rightarrow \infty) = 0$. Explicitly, from the adiabatic charge current in Eq. (28), the meron charge Q_{meron} is given by

$$Q_{\text{meron}} = 1 - \frac{t_2}{\sqrt{m_{\text{AF}}^2 + t_2^2}} \approx \frac{m_{\text{AF}}^2}{2t_2^2}, \quad (36)$$

for SHI phase satisfying $t_2 \gg m_{\text{AF}} > 0$. Similarly for SDW phase which satisfy $m_{\text{AF}} \gg t_2 > 0$,

$$Q_{\text{meron}} = -\frac{t_2}{\sqrt{m_{\text{AF}}^2 + t_2^2}} \approx -\frac{t_2}{m_{\text{AF}}}. \quad (37)$$

Therefore a meron defect has a finite charge, however, which is not quantized.

A meron defect is especially important for the spin ordering with easy-plane anisotropy. Considering a planar antiferromagnetic spin ordering $\mathbf{m}_{\text{AF}} = (m_x, m_y, 0)$, the low energy Hamiltonian can be written as

$$H_{\text{eff},\pm} = \int d^2r \psi_\pm^\dagger(\mathbf{r}, t) [\pm(-i\partial_x)\tau_x + (-i\partial_y)\tau_y + \mu_S\tau_z + \tau_z\{\pm t_2\sigma_z + m_x\sigma_x + m_y\sigma_y\}] \psi_\pm(\mathbf{r}, t), \quad (38)$$

where \pm indicates the two nodes at $\mathbf{k} = \pm\mathbf{K}_1$. After a transformation of $\psi_- \rightarrow \tau_y\sigma_z\psi_-$, the full Hamiltonian $H_{\text{eff}} = H_{\text{eff},+} + H_{\text{eff},-}$ can be written as

$$H_{\text{eff}} = \int d^2r \psi^\dagger(\mathbf{r}, t) [(-i\partial_x)\tau_x + (-i\partial_y)\tau_y + \mu_S\tau_z\nu_z + \tau_z\{t_2\sigma_z + m_x\sigma_x + m_y\sigma_y\}] \psi(\mathbf{r}, t), \quad (39)$$

where $\psi^\dagger = (\psi_+^\dagger, \psi_-^\dagger)$. It is interesting to notice that this Hamiltonian has similar structure as the effective Hamiltonian of CMI derived from AHI in Eq. (7). Now we define a three component unit vector $\hat{N} = \frac{1}{\sqrt{m_x^2 + m_y^2 + t_2^2}}(m_x, m_y, t_2)$ and compute the charge current induced by the adiabatic variation of \hat{N} using the formulation in Sec. III A. A meron can be represented by

$$\hat{N}_{\text{meron}} = (\cos \alpha(r) \cos \phi, \cos \alpha(r) \sin \phi, \sin \alpha(r)), \quad (40)$$

which is under the constraint of $\alpha(r = 0) = \frac{\pi}{2}$ and $\sin[\alpha(r \rightarrow \infty)] = \frac{t_2}{\sqrt{m^2 + t_2^2}}$. Here $m^2 = m_x^2 + m_y^2$, $\phi(\mathbf{r}) = \tan^{-1}(\frac{y}{x})$, and $|\mathbf{r}| = r = \sqrt{x^2 + y^2}$. If $|\mu_S| > \sqrt{m^2 + t_2^2}$, the induced charge is zero. On the other hand, when $|\mu_S| < \sqrt{m^2 + t_2^2}$, the total charge induced by a meron defect is given by

$$Q_{\text{meron}} = \frac{C_S}{4\pi} \int dx dy \hat{N}_{\text{meron}} \cdot [(\partial_x \hat{N}_{\text{meron}}) \times (\partial_y \hat{N}_{\text{meron}})], \\ = \frac{t_2}{\sqrt{m^2 + t_2^2}} - 1, \quad (41)$$

which shows that a meron defect is charged but the net charge is not quantized. $Q_{\text{meron}} \approx \frac{m^2}{2t_2^2}$ for $t_2 \gg m$ while Q_{meron} approaches -1 for $m \gg t_2$. The meron charge of the easy-plane Neel phase derived from SHI is also discussed by the recent work in Ref. 32, in which the same conclusion is obtained.

V. SECOND CHERN NUMBER AND TOPOLOGICAL CONTRIBUTION TO THE INHOMOGENEITY INDUCED ADIABATIC CURRENTS

A. Semiclassical gradient expansion approach for adiabatic currents

In this section, we demonstrate that the charge and spin polarizations induced by the adiabatic variation of the inhomogeneous spin order parameter $N(\hat{\mathbf{r}}, t)$ can be understood as a generic topological response of inhomogeneous systems under adiabatic temporal variations. In particular, it is shown that the topological nature of the adiabatic current of inhomogeneous systems is endowed with the second Chern number. It turns out that the existence of the second Chern number is the topological origin of the fact that the spin and charge polarization quantum induced by the inhomogeneous spin order parameter $N(\hat{\mathbf{r}}, t)$ are determined by the product of two topological invariants, which are defined in the position and momentum spaces, respectively, as shown in Eq. (19) and Eq. (21).

For simplicity, we assume that the system has translational invariance along the x -direction and the spatial inhomogeneity is developed along the y -direction. The total charge current along the x -direction, J_x is given by

$$\begin{aligned} J_x &= \frac{\delta}{\delta A_x} i \text{Tr} \ln G \\ &= -ie \int \frac{dk_x}{2\pi} \int dy \int dt \text{tr} \langle t, y | \hat{G}(k_x) \partial_{k_x} \hat{G}^{-1}(k_x) | t, y \rangle, \end{aligned} \quad (42)$$

where the symbol tr indicates the trace over the discrete indices while Tr includes the trace over discrete indices and integration over the momentum k_x and the position y and time t . Since the electrons are coupled to the time-dependent inhomogeneous order parameter $\hat{N}(y, t)$, the Green's function, which is diagonal in k_x , has off-diagonal components in the (y, t) space, i.e., $\langle y_1, t_1 | \hat{G}(k_x) | y_2, t_2 \rangle = G(k_x; y_1, t_1; y_2, t_2)$.

If $\hat{N}(y, t)$ changes slowly in the position and time spaces, namely, if $L_y \gg 1/E_g$ and $1/T \ll E_g$ are satisfied, the position and time dependence of the Green's function G can be treated by the gradient expansion method. Here L_y (T) is the length (time) scale over which $\hat{N}(y, t)$ varies and E_g is the bulk energy gap. To perform the systematic gradient expansion, we first consider the Wigner transformation of $G(k_x; y_1, t_1; y_2, t_2)$, i.e. the Fourier transformation with respect to the relative coordinates $y_1 - y_2$ and $t_1 - t_2$, which can be written as³³⁻³⁵

$$\begin{aligned} &\tilde{G}(k_x; k_y, \frac{y_1 + y_2}{2}; \omega, \frac{t_1 + t_2}{2}) \\ &\equiv \int d(t_1 - t_2) d(y_1 - y_2) e^{-i[k_y(y_1 - y_2) - \omega(t_1 - t_2)]} \\ &\quad \times G(k_x; y_2, t_1; y_2, t_2). \end{aligned} \quad (43)$$

As shown in detail in the Appendix A, the key ingredient of the gradient expansion is that the Wigner transformed Green's function \tilde{G} can be expanded order by order in powers of

the spatial gradient of the semi-classical Green's function $\mathcal{G}(k_x; k_y, y; \omega, t) = [\omega - \mathcal{H}_{\text{sc}}(k_x; k_y, y; \omega, t)]^{-1}$.^{35,36} In the semi-classical Hamiltonian $\mathcal{H}_{\text{sc}}(k_x; k_y, y; \omega, t)$, the conjugate variables (y, \hat{k}_y) and $(t, \hat{\omega})$ are treated as independent real numbers (y, k_y) and (t, ω) . Here $\hat{k}_y = -i \frac{\partial}{\partial y}$ and $\hat{\omega} = i \frac{\partial}{\partial t}$. Therefore the gradient expansion is equivalent to the semi-classical expansion.

The leading order term of the adiabatic current induced by the spatial inhomogeneity can be written as

$$J_x = J_{x, \text{topological}} + J_{x, \text{perturb}}, \quad (44)$$

in which

$$\begin{aligned} J_{x, \text{topological}} &= -\frac{ie}{60} \int \frac{d\omega}{2\pi} \int_{T^2} \frac{d^2 \mathbf{k}}{(2\pi)^2} \int dy dt \\ &\quad \times \varepsilon_{\nu_1 \nu_2 \nu_3 \nu_4 \nu_5} \text{tr} [\mathcal{G}(\partial_{\nu_1} \mathcal{G}^{-1}) \cdots \mathcal{G}(\partial_{\nu_5} \mathcal{G}^{-1})], \end{aligned} \quad (45)$$

where the indices $(\nu_1, \nu_2, \nu_3, \nu_4, \nu_5)$ run over (ω, k_x, k_y, y, t) . Here T^2 indicates the 2-torus made of two dimensional Brillouin zone. If the (y, t) dependence of the Hamiltonian occurs only through the coupling to $\hat{N}(y, t)$, $J_{x, \text{topological}}$ can be rewritten using the spherical coordinates (θ, ϕ) for the unit vector $\hat{N}(y, t) = \hat{N}(\theta(y, t), \phi(y, t))$ in the following way,

$$\begin{aligned} J_{x, \text{topological}} &= -\frac{ie}{60} \int \frac{d\omega}{2\pi} \int_{T^2} \frac{d^2 \mathbf{k}}{(2\pi)^2} \int_{S^2} d\theta d\phi \\ &\quad \times \varepsilon_{\mu_1 \mu_2 \mu_3 \mu_4 \mu_5} \text{tr} [\mathcal{G}(\partial_{\mu_1} \mathcal{G}^{-1}) \cdots \mathcal{G}(\partial_{\mu_5} \mathcal{G}^{-1})] \\ &= e C_{\text{Chern}}^{(2)} \end{aligned} \quad (46)$$

where the indices $(\mu_1, \mu_2, \mu_3, \mu_4, \mu_5)$ run over $(\omega, k_x, k_y, \theta, \phi)$. When $\hat{N}(y, t)$ fully covers the unit sphere during the adiabatic variation, the total adiabatic current is quantized with the magnitude of the quantum determined by the second Chern number $C_{\text{Chern}}^{(2)}$. All the other non-topological terms, whose contribution would vanish for cyclic evolutions of \hat{N} , are included in $J_{x, \text{perturb}}$. The explicit expressions of $J_{x, \text{perturb}}$ are given in Eq. (A28), Eq. (A29), and Eq. (A30).

The charge density induced by the spatial inhomogeneity can also be derived in a similar way from the semiclassical gradient expansion approach. Starting from the expression of the integrated charge density which is given by

$$\begin{aligned} J_0 &= \frac{\delta}{\delta A_0} i \text{Tr} \ln G \\ &= -ie \int \frac{d\omega}{2\pi} \int dx \int dy \text{tr} \langle x, y | \hat{G}(\omega) \partial_\omega \hat{G}^{-1}(\omega) | x, y \rangle, \end{aligned} \quad (47)$$

the inhomogeneity induced charge can be obtained from the expansion of the Wigner transformed Green's function in the powers of the spatial gradients ∂_x and ∂_y . The lowest order contribution to the adiabatic charge induced by a skyrmion defect appears in the second order terms which contains ∂_x

and ∂_y at the same time. Explicitly, it is given by

$$Q_{\text{skyrmion}} = -\frac{ie}{60} \int \frac{d\omega}{2\pi} \int_{T^2} \frac{d^2\mathbf{k}}{(2\pi)^2} \int_{S^2} d\theta d\phi \times \varepsilon_{\mu_1\mu_2\mu_3\mu_4\mu_5} \text{tr}[\mathcal{G}(\partial_{\mu_1}\mathcal{G}^{-1}) \cdots \mathcal{G}(\partial_{\mu_5}\mathcal{G}^{-1})] \quad (48)$$

where the indices $(\mu_1, \mu_2, \mu_3, \mu_4, \mu_5)$ run over $(\omega, k_x, k_y, \theta, \phi)$. Here θ and ϕ represents the spherical coordinates for the three component unit vector $\hat{N}(x, y) = \hat{N}(\theta(x, y), \phi(x, y))$ describing a skyrmion configuration. The same expression for the skyrmion induced charge was obtained in the recent work by Santos et al. in Ref. 37. It is interesting to notice that Q_{skyrmion} can be obtained simply by replacing the time coordinate t by the spatial coordinate x from the expression of the total adiabatic charge current $J_{x,\text{topological}}$ in Eq. (46).

Now we show that the appearance of the second Chern number in $J_{x,\text{topological}}$ is the topological origin of the fact that the quantum of the pumped charge in CMI is given by the product of two topological invariants as shown in Eq. (19). Let us consider the following semi-classical Green's function \mathcal{G} which describes the low energy excitations of CMIs,³⁸

$$\mathcal{G}^{-1} = \omega - f_1(\mathbf{k})\tau_x - f_2(\mathbf{k})\tau_y - m\tau_z\hat{N}(y, t) \cdot \vec{\sigma}, \quad (49)$$

where $\tau_{x,y,z}$ and $\sigma_{x,y,z}$ are Pauli matrices and $f_{1,2}(\mathbf{k})$ are functions which depend only on the momenta \mathbf{k} . Let us consider the property of the following term,

$$I_{N_a N_b k_1 k_2 \omega} \equiv \text{tr}[\mathcal{G}(\partial_{N_a}\mathcal{G}^{-1})\mathcal{G}(\partial_{N_b}\mathcal{G}^{-1})\mathcal{G}(\partial_{k_1}\mathcal{G}^{-1})\mathcal{G}(\partial_{k_2}\mathcal{G}^{-1})\mathcal{G}(\partial_\omega\mathcal{G}^{-1})], \quad (50)$$

where N_a is a component of the unit vector $\hat{N} = (N_x, N_y, N_z)$. We introduce a local unitary transformation U that satisfies $U^\dagger(\vec{\sigma} \cdot \hat{N})U = \sigma_z$. The semi-classical Green's function in the rotated frame, which is defined as $\mathcal{G}_D \equiv U^\dagger\mathcal{G}U$, is diagonal in the spin $\vec{\sigma}$ space. After inserting the identity $U^\dagger U = 1$ between \mathcal{G} and \mathcal{G}^{-1} , $I_{N_a N_b k_1 k_2 \omega}$ transforms as

$$I_{N_a N_b k_1 k_2 \omega} = \text{tr}[U^\dagger\mathcal{G}(\partial_{N_a}\mathcal{G}^{-1})\mathcal{G}(\partial_{N_b}\mathcal{G}^{-1})U \times \mathcal{G}_D(\partial_{k_1}\mathcal{G}_D^{-1})\mathcal{G}_D(\partial_{k_2}\mathcal{G}_D^{-1})\mathcal{G}_D(\partial_\omega\mathcal{G}_D^{-1})]. \quad (51)$$

Using \mathcal{G} from Eq. (49), it can be shown that

$$U^\dagger\mathcal{G}(\partial_{N_a}\mathcal{G}^{-1})\mathcal{G}(\partial_{N_b}\mathcal{G}^{-1})U = \frac{im^2}{\omega^2 - E^2} \varepsilon_{abc} U^\dagger \sigma_c U. \quad (52)$$

Taking into account the fact that \mathcal{G}_D is spin-diagonal, it can be shown that

$$I_{N_a N_b k_1 k_2 \omega} = \frac{im^2}{\omega^2 - E^2} \varepsilon_{abc} N_c \text{tr}[\sigma_z \mathcal{G}_D(\partial_{k_1}\mathcal{G}_D^{-1})\mathcal{G}_D(\partial_{k_2}\mathcal{G}_D^{-1})\mathcal{G}_D(\partial_\omega\mathcal{G}_D^{-1})], \quad (53)$$

where $E^2 = f_1^2 + f_2^2 + m^2$. Then

$$I_{ytk_1k_2\omega} = \frac{\partial N_a}{\partial y} \frac{\partial N_b}{\partial t} I_{N_a N_b k_1 k_2 \omega} = \frac{im^2}{\omega^2 - E^2} \hat{N} \cdot ((\partial_y \hat{N}) \times (\partial_t \hat{N})) \times \text{tr}[\sigma_z \mathcal{G}_D(\partial_{k_1}\mathcal{G}_D^{-1})\mathcal{G}_D(\partial_{k_2}\mathcal{G}_D^{-1})\mathcal{G}_D(\partial_\omega\mathcal{G}_D^{-1})]. \quad (54)$$

Interestingly, the inhomogeneous part that depends on (y, t) and the homogeneous part that is written in term of \mathcal{G}_D in the (ω, k_x, k_y) space are completely separated. Applying this result to Eq. (45), $J_{x,\text{topological}}$ can be written as

$$J_{x,\text{topological}} = \frac{C_S}{4\pi} \int dy dt \hat{N} \cdot [(\partial_y \hat{N}) \times (\partial_t \hat{N})], \quad (55)$$

where the spin Chern number C_S is defined in terms of \mathcal{G}_D using Eq. (13) after replacing \mathcal{G}_0 by \mathcal{G}_D . It is to be noted that the total charge current $J_{x,\text{topological}}$ induced by the adiabatic change of the spatial inhomogeneity is equal to the net transferred charge, which is shown in Eq. (19). The existence of the topological contribution to the inhomogeneity induced charge current characterized by the second Chern number is the origin of the quantized charge pumping with the quantum of the pumped charge expressed as the product of two distinct topological invariants.

Following the similar line of reasoning, the inhomogeneity induced total spin current can be obtained in the following way,

$$J_{x,\text{topological}}^S = -\frac{ie}{60} \int \frac{d\omega}{2\pi} \int_{T^2} \frac{d^2\mathbf{k}}{(2\pi)^2} \int dy dt \times \varepsilon_{\nu_1\nu_2\nu_3\nu_4\nu_5} \text{tr}[(\frac{\hbar}{2}\vec{\sigma} \cdot \hat{N}(y, t))\mathcal{G}(\partial_{\nu_1}\mathcal{G}^{-1}) \cdots \mathcal{G}(\partial_{\nu_5}\mathcal{G}^{-1})], \quad (56)$$

For the semi-classical Green's function in Eq. (49) it is straightforward to show that,

$$J_{x,\text{topological}}^S = \frac{\hbar C_C}{2 \cdot 4\pi} \int dy dt \hat{N} \cdot [(\partial_y \hat{N}) \times (\partial_t \hat{N})], \quad (57)$$

where C_C is the charge Chern number defined in terms of \mathcal{G} . It is interesting to notice the equivalence of $J_{x,\text{topological}}^S$ above and the total transferred spin S_{transfer} in Eq. (21).

Recently, the topological contribution to the inhomogeneity induced adiabatic charge polarization was investigated by considering the Berry phase approach to the charge polarization.³⁹⁻⁴¹ Using the semiclassical wave packet dynamics formalism, Xiao et al.,^{11,12} have derived the general expression of the adiabatic polarization induced by spatial inhomogeneity. For a 2D multi-band system in which the smooth spatial modulation exists along the β direction ($\beta = x, y$) with the modulation period of L_β , the net charge polarization along the α direction perpendicular to the modulation direction β is given by¹¹⁻¹³,

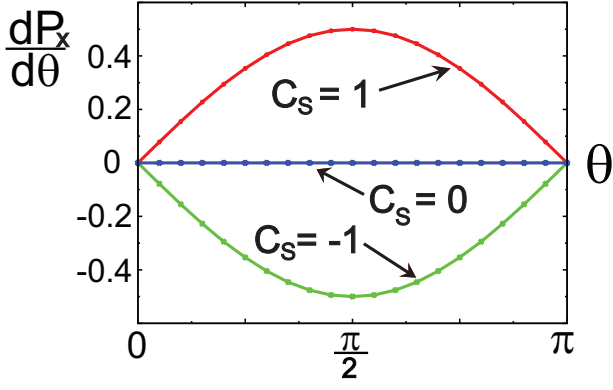


FIG. 8: (Color online) Inhomogeneity induced adiabatic polarization (P_x) for a CMI derived from AHI. A spiral spin ordering with the modulation period of L_y along the y -direction is assumed. $\frac{dP_x}{d\theta}$ is plotted in the unit of e using Eq. (58). For $t_2=2$, $\mu_S=1$, $\frac{dP_x}{d\theta}$ is computed for $m_{AF}=-2, 0.5, 2$ and 4 which correspond to a TCMI ($C_S = -1$), an AHI ($C_S = 0$), another TCMI ($C_S = 1$) and a SDW ($C_S = 0$), respectively. Notice that the polarization is solely determined by the spin Chern number C_S .

$$P_x^{(2)} = \int dr_\beta \int_0^T dt j_\alpha(\mathbf{r}, t),$$

$$= \frac{e}{8} \int dr_\beta \int_{\lambda(0)}^{\lambda(T)} d\lambda \int_{\text{BZ}} \frac{d\mathbf{k}}{(2\pi)^d} \epsilon_{ijkl} \text{Tr}[F_{ij} F_{kl}], \quad (58)$$

where $j_\alpha(\mathbf{r}, t)$ is the inhomogeneity induced adiabatic current as the parameter $\lambda(t)$ evolves from $\lambda(0)$ to $\lambda(T)$. Here the indices i, j, k, l run over $(k_\alpha, k_\beta, r_\beta, \lambda)$ and the Berry curvature F_{ij} satisfies $F_{ij} = \partial_i A_j - \partial_j A_i - i[A_i, A_j]$ with the Berry connection $A_j^{\mu\nu} = \langle \Phi_\mu | i\partial_j | \Phi_\nu \rangle$. Here $|\Phi_\nu\rangle$ is the periodic part of the Bloch wave function for the occupied band ν . The equivalence of the $P_x^{(2)}$ in Eq. (58) and $J_{x,\text{topological}}$ in Eq. (45) can be proved by considering the topological invariance of the second Chern number when the order parameter $\hat{N}(y, t)$ spans a closed manifold. The details of the proof is given in Ref. 4. Therefore the inhomogeneity induced charge polarization can be computed, for a general (lattice) Hamiltonian, using either Eq. (45) or Eq. (58).

B. Adiabatic polarization and skyrmion charge for CMI derived from AHI

To demonstrate the adiabatic polarization induced by inhomogeneous ferrimagnetic ground states, we consider a spiral (or conical) spin ordering pattern with the modulation period $L_y = 2\pi/Q$. The periodic spin modulation along the y direction can also be represented by use of $\hat{N}_{X,Y,Z}^{\text{DW}}$ in Eq. (30) taking $\phi(y) = Qy$. The spatial modulation of the spin ordering is described in Fig. 4. The polarization of the full lattice Hamiltonian \hat{H}_{full} in Eq. (3) is numerically computed from

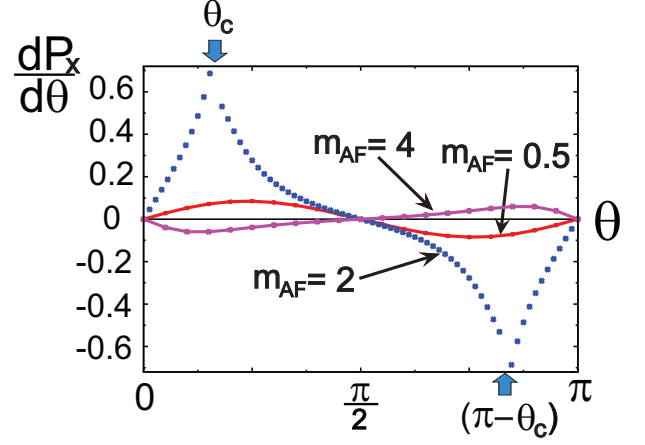


FIG. 9: (Color online) Inhomogeneity induced adiabatic polarization (P_x) for a CMI derived from SHI. A spiral spin ordering with the modulation period of L_y along the y -direction is assumed. $\frac{dP_x}{d\theta}$ is plotted in the unit of e using Eq. (58). For $t_2=2$, $\mu_S=1$, $\frac{dP_x}{d\theta}$ is computed for $m_{AF}=0.5, 2$ and 4 , which are relevant to SHI, TCMI, SDW phases in Fig. 3 (c), respectively, in the collinear limit. $\theta = \theta_c$ and $\theta = (\pi - \theta_c)$ indicate the locations where the singularity in $\frac{dP_x}{d\theta}$ occurs for $m_{AF}=2$.

the second Chern form given in Eq. (58). Since the modulated spin ordering spreads over the whole system, S_z is not conserved any more. Therefore we focus on the charge polarization induced by the inhomogeneous spin ordering.

Let us first consider the CMI derived from AHI. In Fig. 8, we plot the derivative of average polarization $\frac{dP_x}{d\theta}$ per unit modulation period L_y as a function of the polar angle $\theta(\lambda)$ which plays the role of the adiabatic parameter. For $t_2=2$, $\mu_S=1$, the polarization is computed for $m_{AF}=-2, 0.5, 2$ and 4 which, in the collinear limit, correspond to a TCMI ($C_S = -1$), an AHI ($C_S = 0$), another TCMI ($C_S = 1$) and a SDW ($C_S = 0$), respectively, following the phase diagram in Fig. 1 (b). It is worth to be noted that the magnitude and sign of the polarization are solely determined by the spin Chern number C_S . Moreover, as θ evolves from 0 to π , the average polarization per unit modulation period L_y is quantized satisfying $\int_0^\pi d\theta \frac{dP_x}{d\theta} = C_S$. Therefore quantized charge pumping is possible in CMI derived from AHI, consistent with the conclusion in Sec. III. At the same time, this means that a skyrmion defect made of the staggered spin \hat{N} has the charge quantum number C_S . The polarization (or skyrmion charge) is also computed including the ferromagnetic component of the spin order parameter m_F considering the general ferrimagnetic ordering with a net ferromagnetic moment. We have confirmed that m_F does not affect the polarization as long as the bulk band gap is not closed by m_F .

C. Adiabatic polarization and skyrmion charge for CMI derived from SHI

In the case of the CMI derived from SHI, $\frac{dP_x}{d\theta}$ depends on the orientation of the uniform component $\cos\theta$ of the rotating spins relative to the anisotropy direction \mathbf{t}_2 inherent to the SHI. In the case of the spiral ordering described by \hat{N}_X^{DW} or \hat{N}_Y^{DW} in Eq. (30), in which the uniform component aligns perpendicular to the spin anisotropy direction, $\frac{dP_x}{d\theta} = 0$ always. Therefore the net pumped charge is zero in this case.

On the other hand, for the spiral ordering described by \hat{N}_Z^{DW} in Eq. (30), which corresponds to the transverse conical phase with the uniform spin component parallel to \mathbf{t}_2 , $\frac{dP_x}{d\theta}$ is plotted in Fig. 9. For $t_2=2$, $\mu_S=1$, the polarization is computed for $m_{\text{AF}}=0.5, 2$ and 4 , which are relevant to SHI, TCMI, SDW phases in Fig. 3 (c), respectively, in the collinear limit. $\frac{dP_x}{d\theta}$ is odd function with respect to $\theta = \frac{\pi}{2}$, which is consistent with Eq. (33). Because of this, as θ evolves from 0 to π , the net polarization is zero, i.e., $\int_0^\pi d\theta \frac{dP_x}{d\theta} = 0$. Therefore the quantized charge pumping is impossible via the adiabatic rotation of the uniform component of the spiral spins in this case. At the same time, it means that the skyrmion defect has no electric charge independent of $|m_{\text{AF}}|$ in the case of CMI derived from SHI.

The CMIs with $m_{\text{AF}}=2$ satisfy the condition of $|t_2 - \mu_S| < |m_{\text{AF}}| < |t_2 + \mu_S|$, in which the adiabatic polarization could not be properly described by the effective gauge field approach used in Sec. IV. In this case, $\frac{dP_x}{d\theta}$ shows strong enhancement near $\theta = \theta_c$ and $\pi - \theta_c$ as shown in Fig. 9. At the singular points of $\theta = \theta_c$ and $\pi - \theta_c$, $\frac{dP_x}{d\theta}$ is not well-defined. Comparing the magnitude of $\frac{dP_x}{d\theta}$ near $\theta = \theta_c$ or $\theta = \pi - \theta_c$, the partial polarization for $m_{\text{AF}}=2$ is an order of magnitude larger than those for $m_{\text{AF}} = 0.5$ or $m_{\text{AF}} = 4$. The origin of this enhancement can be understood in the following way. The semiclassical Hamiltonian describing the low energy electrons near $\mathbf{k} = \pm\mathbf{K}_1$ in CMI derived from SHI is given by

$$\begin{aligned} \mathcal{H}_{\text{sc}}(\mathbf{k}, \mathbf{r}) &= k_x \tau_x \nu_z + k_y \tau_y + \mu_S \tau_z + t_2 \tau_z \nu_z \sigma_z + m_{\text{AF}} \tau_z \hat{N}(\mathbf{r}, t) \cdot \vec{\sigma}. \end{aligned} \quad (59)$$

Using the semiclassical Green's function $\mathcal{G}^{-1} = \omega - \mathcal{H}_{\text{sc}}$, the local charge Chern number can be defined in the following way,

$$\begin{aligned} C_C(\mathbf{r}, t) &= \frac{\epsilon^{\mu\nu\lambda}}{24\pi^2} \int d^3k \text{Tr} \left[\mathcal{G} \frac{\partial \mathcal{G}^{-1}}{\partial k_\mu} \mathcal{G} \frac{\partial \mathcal{G}^{-1}}{\partial k_\nu} \mathcal{G} \frac{\partial \mathcal{G}^{-1}}{\partial k_\lambda} \right], \\ &= C_+(\mathbf{r}, t) + C_-(\mathbf{r}, t), \end{aligned} \quad (60)$$

in which

$$\begin{aligned} C_\pm(\mathbf{r}, t) &= (\mp) \frac{1}{2} \left[\text{sign} \left(\mu_S + \sqrt{m_{\text{AF}}^2 + t_2^2 \pm 2m_{\text{AF}}t_2N_z} \right) \right. \\ &\quad \left. + \text{sign} \left(\mu_S - \sqrt{m_{\text{AF}}^2 + t_2^2 \pm 2m_{\text{AF}}t_2N_z} \right) \right]. \end{aligned} \quad (61)$$

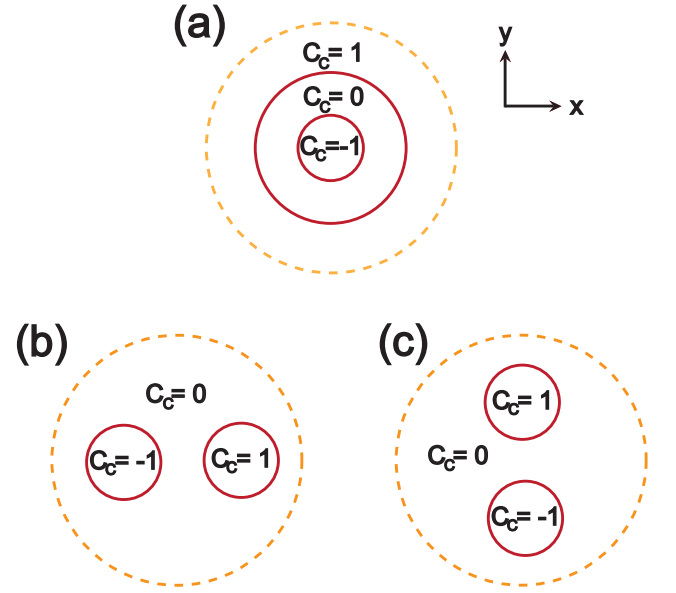


FIG. 10: (Color online) The distribution of local charge Chern numbers within a skyrmion in the case of $(t_2 - \mu_S) < m_{\text{AF}} < (t_2 + \mu_S)$ and $t_2 > \mu_S > 0$. Here the skyrmion configurations for different orientations of \mathbf{m}_{AF} relative to $\mathbf{t}_2 = t_2 \hat{z}$ are considered separately. The largest dotted circle describes the size of a skyrmion. Red solid lines indicate the phase boundary where the charge Chern number changes due to gap-closing. (a) For $\mathbf{m}_{\text{AF}} = m_{\text{AF}} \hat{z}$ ($\mathbf{t}_2 \parallel \mathbf{m}_{\text{AF}}$). (b) For $\mathbf{m}_{\text{AF}} = m_{\text{AF}} \hat{x}$ ($\mathbf{t}_2 \perp \mathbf{m}_{\text{AF}}$). (c) For $\mathbf{m}_{\text{AF}} = m_{\text{AF}} \hat{y}$ ($\mathbf{t}_2 \perp \mathbf{m}_{\text{AF}}$).

In contrast to the cases of $|m_{\text{AF}}| > |t_2 + \mu_S|$ or $|m_{\text{AF}}| < |t_2 - \mu_S|$ in which $C_C(\mathbf{r}, t) = 0$ for any \mathbf{r} and t , when $|t_2 - \mu_S| < |m_{\text{AF}}| < |t_2 + \mu_S|$, $C_C(\mathbf{r}, t)$ changes discontinuously in the (\mathbf{r}, t) space because the energy spectrum of the semiclassical Hamiltonian \mathcal{H}_{sc} develops band touching points. At $\theta = \theta_c$ and $\pi - \theta_c$ where $\frac{dP_x}{d\theta}$ develops singularities, \mathcal{H}_{sc} possesses gapless points at $\mathbf{k} = \mathbf{K}_1$ or $\mathbf{k} = -\mathbf{K}_1$, which is the origin of the strong enhancement of $\frac{dP_x}{d\theta}$. However, since the systems becomes gapless at this point, leakage currents will flow in reality, which disturbs the charge polarization.

The properties of skyrmions in CMI satisfying $|t_2 - \mu_S| < |m_{\text{AF}}| < |t_2 + \mu_S|$ can also be extracted from the spatial distribution of the local charge Chern number $C_C(\mathbf{r}, t) = C_C(x, y)$. We consider the following simple skyrmion configuration,

$$\hat{N}(x, y) = \left(\frac{2x}{x^2 + y^2 + 1}, \frac{2y}{x^2 + y^2 + 1}, \frac{x^2 + y^2 - 1}{x^2 + y^2 + 1} \right), \quad (62)$$

which corresponds to the case of $\mathbf{m}_{\text{AF}} \parallel \mathbf{t}_2$ for $\mathbf{t}_2 = t_2 \hat{z}$. For $(t_2 - \mu_S) < m_{\text{AF}} < (t_2 + \mu_S)$, the local charge Chern number has spatial variation whose distribution is shown in Fig. 10 (a). The red solid circle connects the points where the bulk gap vanishes locally and the Chern number jumps. Due to the occurrence of the gap-closing, the skyrmion defect cannot be constructed from the adiabatic deformation of the spin ordering directions and it is not energetically favorable to make skyrmions in this phase.

Because of the spin anisotropy induced by \mathbf{t}_2 , the distribution of the local charge Chern numbers also depends on the orientation of \mathbf{m}_{AF} . The local Chern number distribution for $\mathbf{t}_2 \perp \mathbf{m}_{\text{AF}}$, which can be described by permuting the components of $\hat{N}(x, y)$ in Eq. (62), are shown in Fig. 10 (b) and (c). The rotation of \mathbf{m}_{AF} relative to \mathbf{t}_2 changes the location of the circles. The size of the solid circle depends on the magnitude of m_{AF} . The topological equivalence of the distribution of the local Chern numbers in Fig. 10 (a), (b), and (c) can be seen after compactifying the boundary of the skyrmion (the dotted circle) into a single point. Therefore a skyrmion configuration always accompanies the band gap-closing.

VI. CONCLUSION

In this work, we have investigated the adiabatic charge and spin polarizations in chiral ferrimagnetic insulators through the smooth tilting of the inhomogeneous spin structures. There are two essential ingredients for the adiabatic polarizations. One is the bulk topological property and the other is the spin anisotropy. In the case of CMI derived from AHI, the charge and spin polarizations are solely determined by the bulk topological properties represented by the charge and spin Chern numbers. The charge and spin Hall effects induced by the spin gauge flux, which can be interpreted as dual responses compared to the usual Hall effects, drive the charge and spin polarizations. Because of its topological nature, quantized pumping is possible and a skyrmion carries quantum numbers in this CMI. In particular, when the system is lack of the spatial inversion symmetry, a new CMI phase dubbed the topological chiral magnetic insulator (TCMI) exists. In TCMI, the quantized charge and spin pumpings are possible and the skyrmion texture is a spin-1/2 fermion with the charge e .

On the other hand, spin anisotropy plays the crucial role in the case of the charge polarization in CMIs derived from SHI. Because of the spin anisotropy induced by the spin-orbit coupling, the charge polarization occurs even in the topologically trivial SDW phases. The charge polarization is also strongly affected by the bulk topological property. When the magnitude of the spin ordering becomes comparable to the spin-orbit coupling strength which corresponds to TCMI phase in the collinear limit, the local charge Chern number changes discontinuously in the position/time spaces. Approaching the local phase boundary where the discontinuity in the local charge Chern number occurs, the charge polarization shows a strong enhancement due to the existence of gap-closing points. In addition, in the case of a meron type defect, it can be charged in contrast to the case of skyrmions. In particular, the meron of the easy-plane Neel state carries finite charge but the net charge is not quantized.

The quantum number of a skyrmion, which exists in CMI derived from TBI (both AHI and SHI) can be summarized in the following way. If the collinear magnetic ground state has finite Chern numbers independent of the spatial orientation of the spins and supports a stable skyrmion defect, the skyrmion carries a nonzero quantum number. In the case of CMI derived from AHI, the relation of the skyrmion quantum

number with Chern numbers of the collinear magnetic ground state is obvious. The charge quantum number of a skyrmion is given by the spin Chern number. On the other hand, the spin quantum number and quantum statistics of a skyrmion are determined by the charge Chern number. In the case of CMI derived from SHI, since the spin Chern number is not well-defined, the topological property of CMI is determined by the charge Chern number. In both SDW and SHI phases, since the charge Chern number is zero, there is no topological contribution to the skyrmion quantum numbers. On the other hand, in the case of TCMI, although it has a finite charge Chern number, a skyrmion is not a stable object because it always accompanies gap-closing. Therefore the stable skyrmion texture of CMI derived from SHI does not carry nonzero quantum numbers, which is consistent with the charge Chern number of the collinear magnetic ground state.

To observe the inhomogeneity induced adiabatic responses, it is necessary to search systems in which both electron correlations and spin-orbit coupling are essential ingredients determining the material properties. Especially, to realize the TCMI, it is required to break lattice inversion symmetry. In this regard, the bilayer of perovskite-type transition-metal oxides grown along the [111] crystallographic axis is a promising playground to realize the TCMI phase because the strength of the inversion symmetry breaking potential can be easily manipulated in this system. The CMI with inhomogeneous spin structures would be a fascinating venue to observe the interplay between the magnetism and electricity coupled through the nontrivial topological invariants.⁴²

This work is supported by the Japan Society for the Promotion of Science (JSPS) through the ‘‘Funding Program for World-Leading Innovative R&D on Science and Technology (FIRST Program)’’.

Appendix A: Adiabatic polarization current from Moyal product expansion

In this Appendix, we explicitly demonstrate how the adiabatic polarization currents of homogeneous/inhomogeneous systems can be derived using the gradient expansion (or Moyal product expansion) method. For the derivation, we have referred the discussions in Ref. 33–36.

1. Polarization current in a system with translational invariance

For a translationally invariant system, the total charge current along the α -direction ($\alpha = x, y$) can be written as

$$J_\alpha = ie \int \frac{d^2 p d\omega}{(2\pi\hbar)^3} \text{tr}[G^{-1}(\mathbf{p}, \omega) \partial_{p_\alpha} G(\mathbf{p}, \omega)], \quad (\text{A1})$$

where the symbol tr denotes the summation over all discrete indices. Throughout this section, we keep the unit \hbar because the gradient expansion is basically equivalent to the semiclassical expansion in powers of \hbar . Let us first consider the adiabatic current induced by the smooth temporal variation of

the system. We assume that the system maintains the translational invariance and the time dependence of the Hamiltonian appears due to the coupling of electrons to the time dependent order parameter field $\hat{N}(t)$. Then the Green's function is, in general, a matrix possessing off-diagonal components in the time space such as $G = G(\mathbf{p}; t, t') \equiv \langle t | \hat{G}(\mathbf{p}) | t' \rangle$. The charge current can also be written as

$$J_\alpha = ie \int \frac{d^2p}{(2\pi\hbar)^2} \int dt \text{tr} \langle t | \hat{G}^{-1}(\mathbf{p}) \partial_{p_\alpha} \hat{G}(\mathbf{p}) | t \rangle. \quad (\text{A2})$$

If the order parameter field $\hat{N}(t)$ changes slowly in time, the time dependence of the Green's function can be treated by using the Wigner transformation. In general, the Wigner transformation of a function $F(t_1, \mathbf{x}_1; t_2, \mathbf{x}_2) \equiv F(x_1; x_2)$ is defined as

$$\tilde{F}(p, R) = \int dr e^{-\frac{i}{\hbar} p \cdot r} F(R + r/2, R - r/2), \quad (\text{A3})$$

where the center-of-mass coordinate $R = \frac{x_1 + x_2}{2}$ and the relative coordinate $r = x_1 - x_2$ with $x_{1,2} = (t_{1,2}, \mathbf{x}_{1,2})$. Also, $p = (\omega, \mathbf{p})$, $p \cdot r = \mathbf{p} \cdot \mathbf{x} - \omega t$. If F is a convolution of two functions such as

$$F(x, z) = \int dy A(x, y) B(y, z). \quad (\text{A4})$$

Then the Wigner transformations of F , A , B , which are represented by \tilde{F} , \tilde{A} , \tilde{B} , respectively, satisfy the following relation,

$$\begin{aligned} \tilde{F}(p, x) &= \tilde{A}(p, x) \tilde{B}(p, x) \\ &- \frac{i\hbar}{2} [(\partial_{p_i} \tilde{A})(\partial_{x_i} \tilde{B}) - (\partial_{x_i} \tilde{A})(\partial_{p_i} \tilde{B})] \\ &- \frac{\hbar^2}{8} [(\partial_{p_i} \partial_{p_j} \tilde{A})(\partial_{x_i} \partial_{x_j} \tilde{B}) + (\partial_{x_i} \partial_{x_j} \tilde{A})(\partial_{p_i} \partial_{p_j} \tilde{B}) \\ &- 2(\partial_{p_i} \partial_{x_j} \tilde{A})(\partial_{x_i} \partial_{p_j} \tilde{B})] + O(\hbar^3). \end{aligned} \quad (\text{A5})$$

It shows that \tilde{F} can be written as a series of the space-time gradients of \tilde{A} and \tilde{B} in which the expansion parameter is given by $\hbar(\frac{\partial}{\partial x_i})(\frac{\partial}{\partial p_i})$. In addition, the trace of F satisfies

$$\text{Tr}[F] = \int dx F(x, x) = \int \frac{dx dp}{(2\pi\hbar)^d} \tilde{A}(p, x) \tilde{B}(p, x), \quad (\text{A6})$$

where d is the space-time dimension.

Using the relation in Eq. (A6), the total charge current J_α (Eq. (A2)) is given by

$$J_\alpha = -ie \int \frac{d^2p}{(2\pi\hbar)^2} \int \frac{dtd\omega}{(2\pi\hbar)} \text{tr}[\tilde{G}(\mathbf{p}, \omega, t) \partial_{p_\alpha} \tilde{K}(\mathbf{p}, \omega, t)], \quad (\text{A7})$$

where \tilde{K} is the Wigner transformation of $K \equiv G^{-1}$ and \tilde{G} is the Wigner transformed Green's function that is defined as

$$\tilde{G}(\mathbf{p}, \omega, t) = \int d(t_1 - t_2) e^{\frac{i}{\hbar} \omega(t_1 - t_2)} G(\mathbf{p}, t_1, t_2), \quad (\text{A8})$$

where $t = (t_1 + t_2)/2$.

For the Hamiltonian \hat{H} which is given by

$$\hat{H} = \int \frac{d\mathbf{p}}{(2\pi\hbar)^2} \psi^\dagger(\mathbf{p}, t) H_0(\mathbf{p}, t) \psi(\mathbf{p}, t), \quad (\text{A9})$$

G and $K = G^{-1}$ satisfy the following relations,

$$\left[i\hbar \frac{\partial}{\partial t_1} - H_0(\mathbf{p}, t_1) \right] G(\mathbf{p}, t_1, t_2) = \hbar \delta(t_1 - t_2), \quad (\text{A10})$$

and

$$\int dt_3 K(\mathbf{p}, t_1, t_3) G(\mathbf{p}, t_3, t_2) = \hbar \delta(t_1 - t_2). \quad (\text{A11})$$

Therefore K is given by

$$\begin{aligned} K(\mathbf{p}, t_1, t_2) &= \left[i\hbar \frac{\partial}{\partial t_1} - H_0(\mathbf{p}, t_1) \right] \delta(t_1 - t_2), \\ &= \int \frac{d\Omega}{2\pi\hbar} \left[\Omega - H_0(\mathbf{p}, \frac{t_1 + t_2}{2}) \right] e^{-\frac{i}{\hbar} \Omega(t_1 - t_2)}. \end{aligned} \quad (\text{A12})$$

After the Wigner transformation of K , we obtain,

$$\tilde{K}(\mathbf{p}, \omega, t) = \omega - H_0(\mathbf{p}, t) \equiv \mathcal{G}^{-1}(\mathbf{p}, \omega, t), \quad (\text{A13})$$

where \mathcal{G} is the semi-classical Green's function in which ω and t are treated as independent variables.

The next step is to express the Wigner transformed Green's function \tilde{G} as a function of the semi-classical Green's function \mathcal{G} . Let us first perform the Wigner transformation of Eq. (A11). From Eq. (A5), we expect that the Wigner transformation of the left hand side of Eq. (A11) can be expanded in powers of \hbar , which leads to following relation,

$$\Theta[\tilde{K}, \tilde{G}] \equiv \sum_{j=0}^{\infty} \hbar^j \Theta_j[\tilde{K}, \tilde{G}] = \hbar, \quad (\text{A14})$$

in which

$$\begin{aligned} \Theta_0[\tilde{K}, \tilde{G}] &= \tilde{K} \tilde{G}, \\ \Theta_1[\tilde{K}, \tilde{G}] &= -\frac{i}{2} [(\partial_{p_i} \tilde{K})(\partial_{x_i} \tilde{G}) - (\partial_{x_i} \tilde{K})(\partial_{p_i} \tilde{G})], \\ \Theta_2[\tilde{K}, \tilde{G}] &= -\frac{1}{8} [(\partial_{p_i} \partial_{p_j} \tilde{K})(\partial_{x_i} \partial_{x_j} \tilde{G}) + (\partial_{x_i} \partial_{x_j} \tilde{K})(\partial_{p_i} \partial_{p_j} \tilde{G}) \\ &- 2(\partial_{p_i} \partial_{x_j} \tilde{K})(\partial_{x_i} \partial_{p_j} \tilde{G})], \end{aligned} \quad (\text{A15})$$

and so on. Now we make expansions of \tilde{G} and \tilde{K} in powers of \hbar in such a way as,

$$\tilde{G} = \sum_{k=0}^{\infty} \hbar^{k+3} \tilde{G}_k, \quad \tilde{K} = \sum_{l=0}^{\infty} \hbar^l \tilde{K}_l, \quad (\text{A16})$$

Putting Eq. (A16) into Eq. (A14), we obtain

$$\Theta_0[\tilde{K}_0, \hbar^3 \tilde{G}_0] = \hbar, \quad (\text{A17})$$

and

$$\sum_{j+k+l>0} \Theta_j[\tilde{K}_l, \tilde{G}_k] = 0, \quad (\text{A18})$$

where the summation is performed for j, k, l for given $j+k+l > 0$. Taking into account of the fact that $\tilde{K} = \tilde{K}_0 = \mathcal{G}^{-1}$, $\tilde{G}_{0,1,2}$ can be obtained as

$$\begin{aligned} \tilde{G}_0 &= \frac{1}{\hbar^2} \mathcal{G}, \\ \tilde{G}_1 &= \frac{i}{2\hbar^2} \mathcal{G}[(\partial_{p_i} \mathcal{G}^{-1})(\partial_{x_i} \mathcal{G}) - (\partial_{x_i} \mathcal{G}^{-1})(\partial_{p_i} \mathcal{G})], \\ \tilde{G}_2 &= \frac{1}{8\hbar^2} \mathcal{G}[(\partial_{p_i} \partial_{p_j} \mathcal{G}^{-1})(\partial_{x_i} \partial_{x_j} \mathcal{G}) + (\partial_{x_i} \partial_{x_j} \mathcal{G}^{-1})(\partial_{p_i} \partial_{p_j} \mathcal{G}) \\ &\quad - 2(\partial_{p_i} \partial_{x_j} \mathcal{G}^{-1})(\partial_{x_i} \partial_{p_j} \mathcal{G})] \\ &\quad + \frac{1}{4\hbar^2} \mathcal{G}(\partial_{x_j} \mathcal{G}^{-1})(\partial_{p_j} [\mathcal{G}(\partial_{p_i} \mathcal{G}^{-1})(\partial_{x_i} \mathcal{G})]) \\ &\quad - \frac{1}{4\hbar^2} \mathcal{G}(\partial_{x_j} \mathcal{G}^{-1})(\partial_{p_j} [\mathcal{G}(\partial_{x_i} \mathcal{G}^{-1})(\partial_{p_i} \mathcal{G})]) \\ &\quad - \frac{1}{4\hbar^2} \mathcal{G}(\partial_{p_j} \mathcal{G}^{-1})(\partial_{x_j} [\mathcal{G}(\partial_{p_i} \mathcal{G}^{-1})(\partial_{x_i} \mathcal{G})]) \\ &\quad + \frac{1}{4\hbar^2} \mathcal{G}(\partial_{p_j} \mathcal{G}^{-1})(\partial_{x_j} [\mathcal{G}(\partial_{x_i} \mathcal{G}^{-1})(\partial_{p_i} \mathcal{G})]). \end{aligned} \quad (\text{A19})$$

Considering a smooth variation of the order parameter field $\hat{N}(t)$ in time, the leading order contribution to \tilde{G} is given by

$$\tilde{G} = \hbar \mathcal{G} - \frac{i\hbar^2}{2} \mathcal{G}[(\partial_\omega \mathcal{G}^{-1})(\partial_t \mathcal{G}) - (\partial_t \mathcal{G}^{-1})(\partial_\omega \mathcal{G})]. \quad (\text{A20})$$

Therefore, from Eq. (A7) and Eq. (A20), the polarization current induced by the adiabatic temporal variation of the order parameter field $\hat{N}(t)$ is given by

$$\begin{aligned} J_\alpha^{(1)} &= -e\hbar^2 \int \frac{d^2 p}{(2\pi\hbar)^2} \int \frac{dt d\omega}{(4\pi\hbar)} \text{tr}[\mathcal{G}\{(\partial_\omega \mathcal{G}^{-1})(\partial_t \mathcal{G}) \\ &\quad - (\partial_t \mathcal{G}^{-1})(\partial_\omega \mathcal{G})\}(\partial_{p_\alpha} \mathcal{G}^{-1})], \\ &= e\hbar^2 \int \frac{d^2 p}{(2\pi\hbar)^2} \int \frac{dt d\omega}{(4\pi\hbar)} \text{tr}[\{(\partial_\omega \mathcal{G}^{-1})\mathcal{G}(\partial_t \mathcal{G}^{-1})\mathcal{G} \\ &\quad - (\partial_t \mathcal{G}^{-1})\mathcal{G}(\partial_\omega \mathcal{G}^{-1})\mathcal{G}\}(\partial_{p_\alpha} \mathcal{G}^{-1})\mathcal{G}], \\ &= e\hbar^2 \int \frac{d^2 p}{(2\pi\hbar)^2} \int \frac{dt d\omega}{(12\pi\hbar)} \\ &\quad \times \varepsilon_{\mu\nu\lambda} \text{tr}[(\partial_\mu \mathcal{G}^{-1})\mathcal{G}(\partial_\nu \mathcal{G}^{-1})\mathcal{G}(\partial_\lambda \mathcal{G}^{-1})\mathcal{G}], \end{aligned} \quad (\text{A21})$$

where (μ, ν, λ) run over (ω, t, p_α) . In particular, considering a cyclic variation of $\hat{N}(t) = \hat{N}(\theta(t))$, which can be parameterized using a polar angle $\theta(t) \in [0, 2\pi]$, the adiabatic current along the x -direction $J_x^{(1)}$, for example, can be written as

$$\begin{aligned} J_x^{(1)} &= e \int \frac{dp_y}{2\pi\hbar} \left\{ \int \frac{dp_x d\theta d\omega}{24\pi^2} \right. \\ &\quad \left. \times \varepsilon_{\mu\nu\lambda} \text{tr}[(\partial_\mu \mathcal{G}^{-1})\mathcal{G}(\partial_\nu \mathcal{G}^{-1})\mathcal{G}(\partial_\lambda \mathcal{G}^{-1})\mathcal{G}] \right\}, \end{aligned} \quad (\text{A22})$$

where $(\mu, \nu, \lambda) = (\omega, \theta, p_x)$. It is interesting to notice that the expression in the large parenthesis $\{\}$ is nothing but the first Chern number, which is the topological origin for the quantized charge pumping through the cyclic variation of the order parameter field $\hat{N}(t)$. The electric charge induced by the one dimensional smooth structure can be described by the same topological invariant if t is replaced by the spatial coordinate x , as discussed in the recent work by Vayrynen et al.⁴³

2. Polarization current in a system with spatial inhomogeneity

Now we consider the adiabatic polarization current in inhomogeneous systems. In particular, we focus on the contribution of the spatial inhomogeneity to the adiabatic current. For simplicity, we assume that the system maintains the translational invariance along the x -direction and the spatial modulation occurs along the y -direction. Using the Wigner transformation, the total charge current of the system can be written as

$$\begin{aligned} J_x &= -ie \int \frac{dp_x}{2\pi\hbar} \int dy \int dt \text{tr}\langle t, y | \hat{G}(p_x) \partial_{p_x} \hat{K}(p_x) | t, y \rangle, \\ &= -ie \int \frac{dp_x}{2\pi\hbar} \int \frac{dy dp_y}{2\pi\hbar} \int \frac{dt d\omega}{2\pi\hbar} \\ &\quad \times \text{tr}[\tilde{G}(p_x; p_y, y; \omega, t) \partial_{p_x} \tilde{K}(p_x; p_y, y; \omega, t)]. \end{aligned} \quad (\text{A23})$$

Smooth variation in the (t, y) space can be treated by using the gradient expansion method following the similar procedures taken in the previous subsection.

We consider a class of Hamiltonians which can be written as

$$\hat{H} = \int \frac{dp_x}{(2\pi\hbar)} \int dy \psi^\dagger(p_x, y, t) H_0(p_x, \frac{\hbar}{i} \frac{\partial}{\partial y}, y, t) \psi(p_x, y, t), \quad (\text{A24})$$

in which H_0 has the dependence on both y and $\frac{\partial}{\partial y}$. The inverse Green's function K is given by

$$\begin{aligned} K(p_x; y_1, t_1; y_2, t_2) &= \left[i\hbar \frac{\partial}{\partial t_1} - H_0(p_x, \frac{\hbar}{i} \frac{\partial}{\partial y_1}, y_1, t_1) \right] \delta(t_1 - t_2) \delta(y_1 - y_2), \\ &= \int \frac{d\Omega dp_y}{(2\pi\hbar)^2} \left[\Omega - H_0(p_x, p_y, \frac{y_1 + y_2}{2}, \frac{t_1 + t_2}{2}) \right] \\ &\quad \times e^{\frac{i}{\hbar} [p_y (y_1 - y_2) - \Omega (t_1 - t_2)]}. \end{aligned} \quad (\text{A25})$$

After the Wigner transformation, \tilde{K} is given by

$$\tilde{K}(p_x; p_y, y; \omega, t) = \omega - H_0(p_x, p_y, y, t) \equiv \mathcal{G}^{-1}, \quad (\text{A26})$$

where \mathcal{G} is the semi-classical Green's function in which (ω, t) and (p_y, y) are treated as independent variables.

To describe the inhomogeneity induced adiabatic current, we consider the gradient expansion of \tilde{G} in powers of \hbar . Since we are interested in the leading order contribution of the spatial inhomogeneity to the adiabatic polarization current, only

the terms which are linear in the derivatives of t and y , respectively, are important. These are included in the \bar{G}_2 in Eq. (A19). The expression of the adiabatic current can be simplified by considering the following relations. At first, $\partial_{p_i}\partial_{p_j}\mathcal{G}^{-1} = \partial_\omega\partial_{p_y}\mathcal{G}^{-1} = 0$ from the general structure of the \mathcal{G} in Eq. (A25). Similarly, $\partial_\omega\partial_t\mathcal{G}^{-1} = \partial_\omega\partial_y\mathcal{G}^{-1} = 0$. Then the leading order contribution to the inhomogeneity induced polarization current can be summarized as

$$J_x^{(2)} = J_x^{(2,A)} + J_x^{(2,B)} + J_x^{(2,C)} + J_x^{(2,D)}, \quad (\text{A27})$$

in which

$$\begin{aligned} J_x^{(2,A)} = & -\frac{ie\hbar^3}{4} \int \frac{dp_x}{2\pi\hbar} \int \frac{dydp_y}{2\pi\hbar} \int \frac{dtd\omega}{2\pi\hbar} \\ & \times \text{tr} \left[\mathcal{G}(\partial_t\partial_y\mathcal{G}^{-1}) \mathcal{G} \left\{ (\partial_\omega\mathcal{G}^{-1}) \mathcal{G}(\partial_{p_y}\mathcal{G}^{-1}) \mathcal{G}(\partial_{p_x}\mathcal{G}^{-1}) \right. \right. \\ & \quad + (\partial_{p_y}\mathcal{G}^{-1}) \mathcal{G}(\partial_\omega\mathcal{G}^{-1}) \mathcal{G}(\partial_{p_x}\mathcal{G}^{-1}) \\ & \quad + (\partial_{p_x}\mathcal{G}^{-1}) \mathcal{G}(\partial_\omega\mathcal{G}^{-1}) \mathcal{G}(\partial_{p_y}\mathcal{G}^{-1}) \\ & \quad + (\partial_{p_x}\mathcal{G}^{-1}) \mathcal{G}(\partial_{p_y}\mathcal{G}^{-1}) \mathcal{G}(\partial_\omega\mathcal{G}^{-1}) \\ & \quad - (\partial_\omega\mathcal{G}^{-1}) \mathcal{G}(\partial_{p_x}\mathcal{G}^{-1}) \mathcal{G}(\partial_{p_y}\mathcal{G}^{-1}) \\ & \quad \left. \left. - (\partial_{p_y}\mathcal{G}^{-1}) \mathcal{G}(\partial_{p_x}\mathcal{G}^{-1}) \mathcal{G}(\partial_\omega\mathcal{G}^{-1}) \right\} \right], \end{aligned} \quad (\text{A28})$$

and

$$\begin{aligned} J_x^{(2,B)} = & \frac{ie\hbar^3}{4} \int \frac{dp_x}{2\pi\hbar} \int \frac{dydp_y}{2\pi\hbar} \int \frac{dtd\omega}{2\pi\hbar} \\ & \times \text{tr} \left[\mathcal{G}(\partial_t\partial_{p_y}\mathcal{G}^{-1}) \mathcal{G} \left\{ (\partial_\omega\mathcal{G}^{-1}) \mathcal{G}(\partial_y\mathcal{G}^{-1}) \mathcal{G}(\partial_{p_x}\mathcal{G}^{-1}) \right. \right. \\ & \quad + (\partial_y\mathcal{G}^{-1}) \mathcal{G}(\partial_\omega\mathcal{G}^{-1}) \mathcal{G}(\partial_{p_x}\mathcal{G}^{-1}) \\ & \quad + (\partial_{p_x}\mathcal{G}^{-1}) \mathcal{G}(\partial_\omega\mathcal{G}^{-1}) \mathcal{G}(\partial_y\mathcal{G}^{-1}) \\ & \quad + (\partial_{p_x}\mathcal{G}^{-1}) \mathcal{G}(\partial_y\mathcal{G}^{-1}) \mathcal{G}(\partial_\omega\mathcal{G}^{-1}) \\ & \quad - (\partial_\omega\mathcal{G}^{-1}) \mathcal{G}(\partial_{p_x}\mathcal{G}^{-1}) \mathcal{G}(\partial_y\mathcal{G}^{-1}) \\ & \quad \left. \left. - (\partial_y\mathcal{G}^{-1}) \mathcal{G}(\partial_{p_x}\mathcal{G}^{-1}) \mathcal{G}(\partial_\omega\mathcal{G}^{-1}) \right\} \right], \end{aligned} \quad (\text{A29})$$

and

$$\begin{aligned} J_x^{(2,C)} = & -\frac{ie\hbar^3}{4} \int \frac{dp_x}{2\pi\hbar} \int \frac{dydp_y}{2\pi\hbar} \int \frac{dtd\omega}{2\pi\hbar} \\ & \times \left\{ \text{tr} \left[\mathcal{G}(\partial_{p_i}\mathcal{G}^{-1}) \mathcal{G} \left\{ (\partial_{p_j}\mathcal{G}^{-1}) \mathcal{G}(\partial_{x_i}\mathcal{G}^{-1}) \right. \right. \right. \\ & \quad + (\partial_{x_i}\mathcal{G}^{-1}) \mathcal{G}(\partial_{p_j}\mathcal{G}^{-1}) \left. \left. \right\} \mathcal{G}(\partial_{p_x}\mathcal{G}^{-1}) \mathcal{G}(\partial_{x_j}\mathcal{G}^{-1}) \right] \\ & + \text{tr} \left[\mathcal{G}(\partial_{x_i}\mathcal{G}^{-1}) \mathcal{G} \left\{ (\partial_{x_j}\mathcal{G}^{-1}) \mathcal{G}(\partial_{p_i}\mathcal{G}^{-1}) \right. \right. \\ & \quad + (\partial_{p_i}\mathcal{G}^{-1}) \mathcal{G}(\partial_{x_j}\mathcal{G}^{-1}) \left. \left. \right\} \mathcal{G}(\partial_{p_x}\mathcal{G}^{-1}) \mathcal{G}(\partial_{p_j}\mathcal{G}^{-1}) \right] \\ & - \text{tr} \left[\mathcal{G}(\partial_{x_i}\mathcal{G}^{-1}) \mathcal{G} \left\{ (\partial_{p_i}\mathcal{G}^{-1}) \mathcal{G}(\partial_{p_j}\mathcal{G}^{-1}) \right. \right. \\ & \quad + (\partial_{p_j}\mathcal{G}^{-1}) \mathcal{G}(\partial_{p_i}\mathcal{G}^{-1}) \left. \left. \right\} \mathcal{G}(\partial_{p_x}\mathcal{G}^{-1}) \mathcal{G}(\partial_{x_j}\mathcal{G}^{-1}) \right] \\ & - \text{tr} \left[\mathcal{G}(\partial_{p_i}\mathcal{G}^{-1}) \mathcal{G} \left\{ (\partial_{x_i}\mathcal{G}^{-1}) \mathcal{G}(\partial_{x_j}\mathcal{G}^{-1}) \right. \right. \\ & \quad \left. \left. + (\partial_{x_j}\mathcal{G}^{-1}) \mathcal{G}(\partial_{x_i}\mathcal{G}^{-1}) \right\} \mathcal{G}(\partial_{p_x}\mathcal{G}^{-1}) \mathcal{G}(\partial_{p_j}\mathcal{G}^{-1}) \right] \left. \right\}, \end{aligned} \quad (\text{A30})$$

and

$$\begin{aligned} J_x^{(2,D)} = & -\frac{ie\hbar^3}{4} \int \frac{dp_x}{2\pi\hbar} \int \frac{dydp_y}{2\pi\hbar} \int \frac{dtd\omega}{2\pi\hbar} \\ & \times \left\{ \text{tr} \left[\mathcal{G}(\partial_{p_x}\mathcal{G}^{-1}) \mathcal{G} \left\{ (\partial_{x_i}\mathcal{G}^{-1}) \mathcal{G}(\partial_{p_i}\mathcal{G}^{-1}) \right. \right. \right. \\ & \quad - (\partial_{p_i}\mathcal{G}^{-1}) \mathcal{G}(\partial_{x_i}\mathcal{G}^{-1}) \left. \left. \right\} \mathcal{G}(\partial_{p_j}\mathcal{G}^{-1}) \mathcal{G}(\partial_{x_j}\mathcal{G}^{-1}) \right] \\ & + \text{tr} \left[\mathcal{G}(\partial_{p_x}\mathcal{G}^{-1}) \mathcal{G} \left\{ (\partial_{p_i}\mathcal{G}^{-1}) \mathcal{G}(\partial_{x_i}\mathcal{G}^{-1}) \right. \right. \\ & \quad \left. \left. - (\partial_{x_i}\mathcal{G}^{-1}) \mathcal{G}(\partial_{p_i}\mathcal{G}^{-1}) \right\} \mathcal{G}(\partial_{x_j}\mathcal{G}^{-1}) \mathcal{G}(\partial_{p_j}\mathcal{G}^{-1}) \right] \left. \right\}, \end{aligned} \quad (\text{A31})$$

where $(x_i, p_i) = (t, \omega)$ or (y, p_y) . Here $J_x^{(2,A)}$ ($J_x^{(2,B)}$) contains the second derivative of \mathcal{G}^{-1} , i.e., $\partial_t\partial_y\mathcal{G}^{-1}$ ($\partial_t\partial_{p_y}\mathcal{G}^{-1}$). $J_x^{(2,C)}$ ($J_x^{(2,D)}$) consists of the terms which contains a symmetric (antisymmetric) permutation of partial derivatives between parenthesis in the middle.

Lattice Dirac Hamiltonian: We apply the above result to the semi-classical lattice Dirac Hamiltonian, which has the following structure,

$$H_{\text{Dirac}} = \sum_{a=1}^5 d_a(\mathbf{p}, \mathbf{x}) \Gamma_a, \quad (\text{A32})$$

in which the five 4×4 traceless Gamma matrices satisfy $\{\Gamma_\mu, \Gamma_\nu\} = 2\delta_{\mu,\nu}\mathbb{I}$ with the identity matrix \mathbb{I} . $\vec{d} = (d_1, d_2, d_3, d_4, d_5)$ is a five-component vector that depends on the position \mathbf{x} and momentum \mathbf{p} coordinates. Using the identity $\text{tr}[\Gamma_i\Gamma_j\Gamma_k\Gamma_l\Gamma_m] = -4\varepsilon_{ijklm}$, it can be shown that

$$J_x^{(2,A)} = J_x^{(2,B)} = 0. \quad (\text{A33})$$

Regarding $J_x^{(2,C)}$ and $J_x^{(2,D)}$, it is crucial to observe the following relation,

$$\begin{aligned} & \int d\omega \text{tr}[\mathcal{G}(\partial_{\nu_1}\mathcal{G}^{-1}) \cdots \mathcal{G}(\partial_{\nu_5}\mathcal{G}^{-1})] \\ & = \int d\omega \frac{1}{120} \varepsilon_{\nu_1\nu_2\nu_3\nu_4\nu_5} \text{tr}[\mathcal{G}(\partial_{\nu_1}\mathcal{G}^{-1}) \cdots \mathcal{G}(\partial_{\nu_5}\mathcal{G}^{-1})], \end{aligned} \quad (\text{A34})$$

where the five indices $(\nu_1, \nu_2, \nu_3, \nu_4, \nu_5)$ run over (ω, p_x, p_y, t, y) . The antisymmetry of the trace under the permutation of the indices ν_i leads to

$$J_x^{(2,C)} = 0, \quad (\text{A35})$$

and

$$\begin{aligned} J_x^{(2,D)} = & -\frac{ie\hbar^3}{60} \int \frac{dp_x}{2\pi\hbar} \int \frac{dydp_y}{2\pi\hbar} \int \frac{dtd\omega}{2\pi\hbar} \\ & \times \varepsilon_{\nu_1\nu_2\nu_3\nu_4\nu_5} \text{tr}[\mathcal{G}(\partial_{\nu_1}\mathcal{G}^{-1}) \cdots \mathcal{G}(\partial_{\nu_5}\mathcal{G}^{-1})]. \end{aligned} \quad (\text{A36})$$

For the description of the charge pumping in topological chiral magnets, we can assume that the spatial inhomogeneity of the system appears only through the coupling to the inhomogeneous order parameter field $\hat{N}(y, t)$ and the charge current is induced by the adiabatic variation of $\hat{N}(y, t)$, which

satisfies $\hat{N}^2 = 1$, i.e., $\hat{N} \in S^2$. We introduce a spherical coordinate (θ, ϕ) for the space-time (y, t) dependent unit vector field $\hat{N}(y, t) = \hat{N}(\theta(y, t), \phi(y, t))$. Then $J_x^{(2,D)}$ can be rewritten as

$$\begin{aligned} J_x^{(2,D)} &= -\frac{ie}{60} \int \frac{d\omega}{2\pi} \int_{T^2} \frac{d^2\mathbf{p}}{(2\pi)^2} \int_{S^2} d\Omega(\theta, \phi) \\ &\quad \times \varepsilon_{\mu_1\mu_2\mu_3\mu_4\mu_5} \text{tr}[\mathcal{G}(\partial_{\mu_1}\mathcal{G}^{-1}) \cdots \mathcal{G}(\partial_{\mu_5}\mathcal{G}^{-1})], \\ &= eC_{\text{Chem}}^{(2)}, \end{aligned} \quad (\text{A37})$$

where the indices $(\mu_1, \mu_2, \mu_3, \mu_4, \mu_5)$ run over $(\omega, p_x, p_y, \theta, \phi)$. Here T^2 indicates the 2-torus given by two dimensional Brillouin zone. It is interesting to note that $C_{\text{Chem}}^{(2)}$ is nothing but the second Chern number, which

is quantized when the spherical solid angle $\Omega(\theta, \phi)$ is fully covered by $\hat{N}(y, t)$. Therefore the inhomogeneity induced adiabatic current $J_x^{(2)}$ can be summarized in the following suggestive way,

$$J_x^{(2)} = J_{x,\text{topological}}^{(2)} + J_{x,\text{perturb}}^{(2)}, \quad (\text{A38})$$

in which $J_{x,\text{topological}}^{(2)} = J_x^{(2,D)}$ is the topological contribution to the adiabatic current whose topological nature is endowed with the second Chern number. All the other non-topological (perturbative) contributions are included in $J_{x,\text{perturb}}^{(2)} = J_x^{(2,A)} + J_x^{(2,B)} + J_x^{(2,C)}$.

-
- ¹ R. Jackiw and C. Rebbi, Phys. Rev. D **13**, 3398 (1976).
² W. P. Su, J. R. Schrieffer, and A. J. Heeger, Phys. Rev. B **22**, 2099 (1980).
³ J. Goldstone and F. Wilczek, Phys. Rev. Lett. **47**, 986 (1981).
⁴ X.-L. Qi, T. L. Hughes, and S.-C. Zhang, Nature Phys., **4**, 273 (2008); X.-L. Qi, T. L. Hughes, and S.-C. Zhang, Phys. Rev. B **78**, 195424 (2008).
⁵ S. Murakami, N. Nagaosa, and S.-C. Zhang, Phys. Rev. Lett. **93**, 156804 (2004).
⁶ F. D. M. Haldane, Phys. Rev. Lett. **61**, 2015 (1988).
⁷ C. L. Kane and E. J. Mele, Phys. Rev. Lett. **95**, 226801 (2005); J. E. Moore and L. Balents, Phys. Rev. B **75**, 121306(R) (2007); R. Roy, Phys. Rev. B **79**, 195321 (2009); B. A. Bernevig, T. L. Hughes, and S.-C. Zhang, Science, **314**, 1757 (2006); M. Koenig, S. Wiedmann, C. Bruene, A. Roth, H. Buhmann, L. W. Molenkamp, X. L. Qi, and S.-C. Zhang, Science, **318**, 766 (2007).
⁸ D.-H. Lee, G.-M. Zhang, T. Xiang, Phys. Rev. Lett. **99**, 196805 (2007); Y. Ran, A. Vishwanath, D.-H. Lee, Phys. Rev. Lett. **101**, 086801 (2008); X.-L. Qi and S.-C. Zhang, Phys. Rev. Lett. **101**, 086802 (2008).
⁹ S. Raghu, X.-L. Qi, C. Honerkamp and S.-C. Zhang, Phys. Rev. Lett. **100**, 156401 (2008).
¹⁰ T. Grover and T. Senthil, Phys. Rev. Lett. **100**, 156804 (2008).
¹¹ D. Xiao, J. Shi, D. P. Clougherty, and Q. Niu, Phys. Rev. Lett. **102**, 087602 (2009).
¹² D. Xiao, M.-C. Chang, and Q. Niu, Rev. Mod. Phys. **82**, 1959 (2010).
¹³ A. M. Essin, J. E. Moore, and D. Vanderbilt, Phys. Rev. Lett. **102**, 146805 (2009).
¹⁴ B. J. Kim, H. Jin, S. J. Moon, J.-Y. Kim, B.-G. Park, C. S. Leem, Jaejun Yu, T. W. Noh, C. Kim, S.-J. Oh, J.-H. Park, V. Durairaj, G. Cao, and E. Rotenberg, Phys. Rev. Lett. **101**, 076402 (2008).
¹⁵ B. J. Kim, H. Ohsumi, T. Komesu, S. Sakai, T. Morita, H. Takagi, T. Arima, Science **323**, 1329 (2009).
¹⁶ S. J. Moon, H. Jin, W. S. Choi, J. S. Lee, S. S. A. Seo, J. Yu, G. Cao, T. W. Noh, and Y. S. Lee, Phys. Rev. B **80**, 195110 (2009).
¹⁷ H. Jin, H. Jeong, T. Ozaki, and J. Yu, Phys. Rev. B **80**, 075112 (2009).
¹⁸ A. Shitade, H. Katsura, J. Kunes, X.-L. Qi, S.-C. Zhang, and N. Nagaosa, Phys. Rev. Lett. **102**, 256403 (2009).
¹⁹ D. Xiao, W. Zhu, Y. Ran, N. Nagaosa, and S. Okamoto, arXiv:1106.4296 (unpublished).
²⁰ K.-Y. Yang, W. Zhu, D. Xiao, S. Okamoto, Z. Wang, and Y. Ran, arXiv:1109.1551 (unpublished).
²¹ D. J. Thouless, M. Kohmoto, M. P. Nightingale, and M. den Nijs, Phys. Rev. Lett. **49**, 405 (1982).
²² M. Kohmoto, Ann. Phys. (N.Y.) **160**, 343 (1985).
²³ M. Mostovoy, Phys. Rev. Lett. **96**, 067601 (2006).
²⁴ V. M. Yakovenko, arXiv: cond-mat/9703195 (unpublished); G. E. Volovik and V. M. Yakovenko, J. Phys. Condens. Matter **1**, 5263 (1989); V. M. Yakovenko, Phys. Rev. Lett. **65**, 251 (1990).
²⁵ K. Sengupta and V. M. Yakovenko, Phys. Rev. B **62**, 4586 (2000); K. Sengupta, R. Roy, and M. Maiti, Phys. Rev. B **74**, 094505 (2006).
²⁶ F. Wilczek and A. Zee, Phys. Rev. Lett. **51**, 2250 (1983).
²⁷ J. C. Y. Teo and C. L. Kane, Phys. Rev. B **82**, 115120 (2010).
²⁸ Y. Tokura and S. Seki, Adv. Mater. **22**, 1554 (2010).
²⁹ H. Katsura, N. Nagaosa, and A. V. Balatsky, Phys. Rev. Lett. **95**, 057205 (2005).
³⁰ M. A. H. Vozmediano, M. I. Katsnelson, and F. Guinea, Phys. Rep. **496**, 109 (2010).
³¹ B.-J. Yang and H.-Y. Kee, Phys. Rev. B **82**, 195126 (2010).
³² D.-H. Lee, Phys. Rev. Lett. **107**, 166806 (2011).
³³ J. Rammer and H. Smith, Rev. Mod. Phys. **58**, 323 (1986).
³⁴ V. Gurarie, Phys. Rev. B **83**, 085426 (2011).
³⁵ G. A. Baraff and S. Borowitz, Phys. Rev. **121**, 1704 (1961).
³⁶ G. E. Volovik, The Universe in a Helium Droplet (Oxford University Press, Oxford, 2003).
³⁷ L. Santos, Y. Nishida, C. Chamon, and C. Mudry, Phys. Rev. B **83**, 104522 (2011).
³⁸ Compared to the low energy Hamiltonians for TCMI's in Eq. (7) and Eq. (23), the inversion symmetry breaking term (μ_S) is missing in this semi-classical Green's function. However, as long as the the inversion symmetry breaking term does not induce bulk band gap-closing, the topological property of the system can still be described with given \mathcal{G} here.
³⁹ R. D. King-Smith and D. Vanderbilt, Phys. Rev. B **47**, 1651 (1993).
⁴⁰ R. Resta, Rev. Mod. Phys. **66**, 899 (1994).
⁴¹ G. Ortiz and R. M. Martin, Phys. Rev. B **49**, 14202 (1994).
⁴² R. Shindou and N. Nagaosa, J. Phys. Soc. Jpn. **74**, 2361 (2005).
⁴³ J. I. Väyrynen and G. E. Volovik, JETP Lett. **93**, 344 (2011).